Anonymous Referee #4

General comments

I thank the authors for their efforts in revising the paper, and in particular including the new Fig. 11. This figure indicates that the enhancement of snow albedo reduction associated with internal mixing of dust in snow as compared with external mixing is typically 28% for the effective medium approximation used by the authors and 16% for the geometric-optics surface-wave approach. Whether or not this is a small difference is a matter of taste, but the main point is that this difference is now adequately documented. I recommend the acceptance of this paper in ACP subject to a small number of minor comments, as given below.

R: We are very grateful for the referee's positive comments. The followings are our point-by-point responses to the comments. Our responses start with "R:". In addition, we also updated Figure 5 due to the previous misuse of Figure 5a.

Minor comments

1. p.14, lines 11–13: "For example, the α_λ decreased by 0.6%, 1.4% and 1.4% . . . for dust concentrations of 2, 10, and 100 ppm respectively". The latter 1.4% is a typo? Fig. 6d suggests that snow albedo decreases from about 0.89 to 0.85.

R: Sorry for this mistake and we have revised as "For example, the α_λ decreased by 0.6%, 1.4%, and 4.7% . . . for dust concentrations of 2, 10, and 100 ppm respectively". Meanwhile, we also rechecked other relevant values throughout the manuscript.

2. p. 17, lines 12–14: "it should be emphasized that the uncertainty of $E_{\alpha,\ integrated}$ induced by dust size comes purely from the uncertainty of broadband albedo of dust-snow external mixing due to different dust sizes". This sentence can easily be interpreted so that in the case of internal mixing, there is no albedo uncertainty associated with dust size. But this is only an artifact of your approach. In reality, it is virtually certain that snow albedo depends on dust particle size also for the case of internal dust-snow mixing.

So it would be more appropriate to say something like: "This uncertainty estimate accounts only for the impact of dust size on snow albedo in the case of external mixing, since the impact on albedo due to dust size cannot be evaluated when using the effective medium approximation." (In fact, it might be speculated that a change in dust particle size would change the snow albedo in the same direction both for external and internal mixing — and therefore, the uncertainty in $E_{\alpha,\ integrated}$ (i.e., the ratio of albedo for internal vs. external mixing) could be smaller than calculated here.)

R: Revised as suggestion in p.17, line 5-8: "it should be emphasized that this uncertainty estimate accounts only for the impact of dust size on snow albedo in the case of external mixing, since the impact on albedo due to dust size cannot be evaluated when using the effective medium approximation. "

3. p. 17, line 18: uncertainties of ±11.0% and ±11.2% are reported for the ratio of $\alpha_{integrated}$ for internal vs. external snow-dust mixing. This sounds like quite a large uncertainty. What was assumed about snow grain size and dust concentration? I would assume the uncertainties are largest when snow grains are large and the dust concentration is high.

R: We have added more details about the uncertainties in p.17, line 8-12: "Overall, the total uncertainty of $E_{\alpha,\ integrated}$ from variations of imaginary RIs and dust diameter was ±11.0% and ±11.2% for IDM (uniform) and IDM (central, $\bar{r}_c$ <0.75), respectively, with dust mass concentrations of 0–100 ppm and r_{ef} of 50–1000 µm. Specifically, the uncertainty increased with increasing r_{ef} and dust concentrations."

1 **Enhanced light absorption and reduced snow albedo due to**

2 **internally mixed mineral dust in grains of snow**

3 Tenglong Shi[1], Jiecan Cui[1], Yang Chen[1], Yue Zhou[1], Wei Pu[1], Xuanye Xu[2], Quanliang

4 Chen[2], Xuelei Zhang[3], and Xin Wang[1,4]

5 [1]Key Laboratory for Semi-Arid Climate Change of the Ministry of Education, College

6 of Atmospheric Sciences, Lanzhou University, Lanzhou 730000, China

7 [2]College of Atmospheric Sciences, Chengdu University of Information Technology,

8 Chengdu 610225, China

9 [3]Key laboratory of Wetland Ecology and Environment, Northeast Institute of

10 Geography and Agroecology, Chinese Academy of Sciences, Changchun 130102,

11 China

12 [4]Institute of Surface-Earth System Science, Tianjin University, Tianjin 300072, China

14 Corresponding author: Xin Wang (wxin@lzu.edu.cn)

Abstract. Mineral dust is a major light-absorbing aerosol, which can significantly reduce snow albedo and accelerate snow/glacier melting via wet and dry deposition on snow. In this study, three scenarios of internal mixing of dust in ice grains were analyzed theoretically by combining asymptotic radiative transfer theory and (core/shell) Mie theory to evaluate the effects on absorption coefficient and albedo of the semi-infinite snowpack consisting of spherical snow grains. In general, snow albedo was substantially reduced at wavelengths of <1.0 μm by internal dust–snow mixing, with stronger reductions at higher dust concentrations and larger snow grain sizes. Moreover, calculations showed that a non-uniform distribution of dust in snow grains can lead to significant differences in the values of the absorption coefficient and albedo of dust-contaminated snowpack at visible wavelengths relative to a uniform dust distribution in snow grains. Finally, using comprehensive in situ measurements across the Northern Hemisphere, we found that broadband snow albedo was further reduced by 5.2% and 9.1% due to the effects of internal dust–snow mixing on the Tibetan Plateau and North American mountains. This was higher than the reduction in snow albedo caused by black carbon in snow over most North American and Arctic regions. Our results suggest that significant dust–snow internal mixing is important for the melting and retreat of Tibetan glaciers and North American mountain snowpack.

1. Introduction

Snow cover is one of the most reflective surfaces in the Earth system, and plays a crucial role in the atmospheric solar radiation energy budget via snow albedo feedbacks (Di Mauro et al., 2020; Flanner et al., 2011; Jacobson, 2004; Usha et al., 2020; Xie et al., 2018). Previous studies have shown that light-absorbing particles (LAPs) effectively reduce snow albedo and enhance the absorption of solar radiation after deposition, these studies were based on in situ observations and model simulations (Casey et al., 2017; Hadley and Kirchstetter, 2012; Shi et al., 2020; Warren and Wiscombe, 1980; Yasunari et al., 2012; Yasunari et al., 2015). As a result, snow contaminated with LAPs shows significant changes in morphology (Niwano et al., 2012; Rango et al., 1996), chemistry (France et al., 2012; Reay et al., 2012), hydrology (Matt et al., 2018; Qian et al., 2015; Rahimi et al., 2019), snowmelt rate (Kaspari et al., 2015; Warren, 1984;), and radiative properties (Grenfell et al., 2002; Hansen and Nazarenko, 2004; Zhao et al., 2014).

Numerous studies have assessed the potential effects of LAPs, such as black carbon (BC) and mineral dust, on snow albedo by assuming that LAPs mixed outside spherical snow grains (i.e., external mixing) (Flanner et al., 2007; Kokhanovsky, 2013; Libois et al., 2013; Wang et al., 2017; Warren and Wiscombe, 1980). For example, Warren and Wiscombe (1980) calculated snow spectral albedo by solving a radiative transfer equation using Mie theory and δ-Eddington approximations, and found that 10–100 ng g^{-1} of BC and 1–10 µg g^{-1} of dust in old snow decreased albedo by 1%–7% and 2%–10% at 400 nm wavelength, respectively. Flanner et al. (2007) pointed out that the reduction in snow albedo for 1000 ng g^{-1} BC in snow was 0.045 (0.17) with a 50 (1000) µm snow grain radius (R_{ef}) based on the Snow, Ice, and Aerosol Radiation (SNICAR) radiative transfer model. This model utilizes theory from Wiscombe and Warren (1980) and the two-stream radiative transfer solution from Toon et al. (1989). Wang et al. (2017) developed a Spectral Albedo Model for Dirty Snow (SAMDS) based on asymptotic radiative transfer theory, which is a function of the snow grain radius, LAP (e.g., BC, dust) mixing ratios, and the mass absorption coefficients (MACs) of LAPs. Their results

1   revealed that broadband snow albedo decreased 0.03 and 0.003 due to 200 ng g^{-1} of BC

2   and 2 μg g^{-1} of dust in snow, respectively, with a R$_{ef}$ of 200 μm. Additionally, recent

3   studies found that snow nonsphericity can interact with LAP-snow mixing, which leads

4   to weaker LAP-induced albedo reductions for nonspherical snow shapes than snow

5   spheres (e.g., Dang et al., 2016; He et al., 2018, 2019).

6   Recently, direct snowpack observations have shown evidence for the existence of LAP–

7   snow internal mixing (e.g., Horhold et al., 2012; Spaulding et al., 2011). LAPs tend to

8   mix externally with snow grains through dry deposition and/or below cloud scavenging,

9   while internal LAP–snow mixing can be produced by nucleation, accretion, riming,

10   aggregation, and sintering during aerosol–cloud–precipitation processes (i.e., wet

11   deposition; Figure 1) (Flanner et al., 2012). Furthermore, Flanner et al. (2012) found

12   that internal BC/ice mixing (IBM) increased the absorption of snowpack by a factor

13   1.8–2.1 relative to external BC/ice mixing (EBM). He et al. (2018) indicated that IBM

14   enhanced the mean snow albedo reduction over the Tibetan plateau by 30%–60%

15   relative to EBM, based on the updated SNICAR model. Additionally, Dombrovsky and

16   Kokhanovsky (2020) demonstrated that non-uniform BC distribution in ice grains may

17   lead to significantly different absorption coefficients and snowpack albedo in visible

18   (VIS) wavelengths.

19   Numerous studies have addressed the role of IBM in enhancing the absorption of

20   snowpack due to its strong absorption effect relative to other LAPs (Dombrovsky and

21   Kokhanovsky, 2020; Flanner et al., 2012; He et al., 2018; Liou et al., 2011). In contrast,

22   few studies have considered the effects of internal dust/ice mixing (IDM) in snowpack.

23   Liou et al. (2014) is the pioneer to investigate the dust-snow internal mixing effects

24   based on the geometric-optics surface-wave approach. Subsequently, He et al. (2019)

25   used the same method to explicitly quantify the combined effects of dust-snow internal

26   mixing and snow grain nonsphericity on snow optical properties, thereafter, develop a

27   set of new dust-snow parameterizations for land/climate modeling applications for the

28   first time. Actually, dust particles are generally larger than BC, and act as more efficient

1 ice nuclei, showing a better ability to influence cloud formation and precipitation

2 (Creamean et al., 2013; Huang et al., 2014). Therefore, they are more likely to mix

3 internally with ice grains. Furthermore, dust can also dominate light absorption and

4 effectively decrease snow albedo because of its relatively high mass abundance (ppm)

5 in snowpack, especially in areas with seasonal and patchy snow cover or mountainous

6 regions (Di Mauro et al., 2015; Gabbi et al., 2015; Painter et al., 2012; Reynolds et al.,

7 2020; Xie et al., 2018). Therefore, it is important to account for IDM when estimating

8 the impact of dust deposition on snow albedo.

9 In this study, we assess the effects of external/internal mixing of dust with ice grains on

10 the snowpack absorption coefficient and albedo using asymptotic radiative transfer

11 theory and Mie theory. In addition, the uniformity and nonuniformity of dust particle

12 distribution inside ice grains are considered for IDM based on the effective medium

13 approximation, and the combined effects of dust content and snow grain radius on snow

14 albedo are quantified. A schematic of various dust spatial distributions from this study

15 is presented in Figure 2. We further discuss snow albedo sensitivity to complex

16 refractive indices and dust particle size distribution. Based on a comprehensive set of

17 field measurements of dust concentrations, we estimate the reductions in snow albedo

18 by dust external/internal mixing with ice grains across the Northern Hemisphere.

19 **2 Methods**

20 **2.1 External mixing model**

21 For fairly pure snow, semi-infinite means about 20 cm in the VIS and 3 cm in the near-

22 infrared (NIR) regions of snow depths, respectively (Zhou et al., 2003). For a semi-

23 infinite snow layer under diffuse illumination conditions, albedo can be calculated

24 using an asymptotic analysis of radiative transfer theory, which is valid in small

25 absorptions (Kokhanovsky and Zege, 2004; Zege et al., 1991):

26 $\alpha_\lambda = exp\,(-4S_\lambda)$ (1)

27 where α_λ is the spectral snow albedo, λ is the wavelength, S_λ is the similarity

1   parameter, and

2    $$S_\lambda = \sqrt{\frac{\sigma_{abs}}{3\sigma_{ext}(1-g)}} \qquad (2)$$

3   In Eq. (2), σ_{abs} and σ_{ext} are the absorption and extinction coefficients, respectively,

4   and g is the asymmetry parameter (the average cosine of the phase function of the

5   medium).

6   According to Eq. (18) and (25) in Kokhanovsky and Zege (2004), the extinction

7   coefficients of particles can be expressed as:

8    $$\sigma_{ext} = \frac{1}{l_{tr}(1-g)} = \frac{3C_v}{2r_{ef}} \qquad (3)$$

9   where l_{tr} is the photon transport path length, $C_v = \rho_{snow}/\rho_{ice}$ is the volumetric

10   snow particle concentration, and the values $\rho_{ice} = 916.7 \text{ kg m}^{-3}$ and $\rho_{snow} = 300 \text{ kg}$

11   m^{-3} are used in subsequent calculations. r_{ef} is the effective snow grain radius, which

12   is equal to the radius of the volume-to-surface equivalent sphere ($r_{ef} = \frac{3\overline{V}}{4\overline{A}}$) where $\overline{V}$

13   and $\overline{A}$ are the average volume and cross-sectional (geometric shadow) area of snow

14   grains, respectively.

15   For external dust/ice mixing (EDM) in a dust-contaminated snowpack, the total

16   absorption coefficient (σ_{abs}) can be derived from the absorptions by snow (σ_{abs}^{snow}) and

17   dust (σ_{abs}^{dust}):

18   $$\sigma_{abs} = \sigma_{abs}^{snow} + \sigma_{abs}^{dust} \qquad (4)$$

19   For example, consider a hypothetical case of snow composed of monodispersed,

20   spherical grains of ice. Although non-spherical snow grains lead to a slight increase in

21   snow albedo, Dang et al. (2016) found that the albedo of a snowpack consisting of non-

22   spherical snow grains can be mimicked by using smaller, spherical grains; thus, we do

23   not consider the effect of non-spherical snow grains in this study. Therefore, we used

24   the following equation for the absorption coefficient of snow (Dombrovsky and Baillis,

25   2010):

26   $$\sigma_{abs}^{snow} = \frac{0.75 C_v \cdot Q_{abs}^{ice}}{r_{ef}} \qquad (5)$$

27   where Q_{abs}^{ice} is the efficiency factor of absorption for a single ice grain, and the value

1   of Q_{abs}^{ice} can be calculated for homogeneous spherical ice grains considered in classical

2   Mie theory.

3   The absorption coefficient of dust (Aoki et al., 2000; Marley et al., 2001; Warren et al.,

4   2006) is expressed as:

5    $$\sigma_{abs}^{dust} = \frac{Q_{abs}^{dust} \cdot \pi \cdot \left(r_{ef}^{dust}\right)^2}{\frac{4}{3}\pi \cdot \left(r_{ef}^{dust}\right)^3} \cdot C_{dust} = \frac{3Q_{abs}^{dust}}{4r_{ef}^{dust}} \cdot C_{dust} = MAC_{abs}^{dust} \cdot \rho_{dust} \cdot C_{dust} \qquad (6)$$

6   where Q_{abs}^{dust} and MAC_{abs}^{dust} is the absorption efficiency and MAC of dust,

7   respectively, that can be obtained via Mie theory, and ρ_{dust} and r_{ef}^{dust} represent the

8   density and effective dust radius, respectively. In this study, ρ_{dust} was assumed to be

9   2500 kg m^{-3} (Zender et al., 2003). We also assumed a log-normal dust size distribution

10   with a geometric mean diameter of 0.65 μm and standard deviation of 2.0 (equivalent

11   to an effective radius of 1.1 μm), which represents dust from large-scale transport

12   (Formenti et al., 2011; Maring et al., 2003) that is likely smaller in size than from local

13   soil (Kok, 2011). The effects of dust size on snow optical properties and albedo were

14   further quantified through sensitivity simulations (see section 3.4). Dust volumetric

15   concentrations (C_{dust}) are expressed as:

16   $$C_{dust} = \frac{\rho_{snow} \cdot C_{dust}^*}{\rho_{dust}} \qquad (7)$$

17   where C_{dust}^* is the mass concentration of dust in snow (kg kg^{-1}). Thus, the spectral

18   albedo of dust-contaminated snow for EDM can be easily calculated with Eq. (1) to (7).

19   **2.2 Internal mixing model**

20   For the IDM (Figure 2), we first determined the effective optical constants of ice

21   containing small dust particles via an effective medium approximation (Maxwell-

22   Garnett and Larmor, 1904). According to this approach, the complex permittivity of a

23   composite medium in ice grains can be calculated in terms of particle polarizability by

24   applying the Lorentz-Lorenz formula (Koledintseva et al., 2009; Markel, 2016). We

25   used the following relationships to calculate effective complex refractive indices (RIs),

26   $m_{ef} = n_{ef} - ik_{ef}$ at known values of $m_{ice} = n_{ice} - ik_{ice}$ for pure ice and $m_{dust} = n_{dust} - ik_{dust}$

for dust:

$$m_{ef}^2 = m_{ice}^2 \frac{2\delta_{dust}(m_{dust}^2 - m_{ice}^2) + m_{dust}^2 + 2m_{ice}^2}{2m_{ice}^2 + m_{dust}^2 - \delta_{dust}(m_{dust}^2 - m_{ice}^2)} \tag{8}$$

where δ_{dust} is the local dust fraction volume in an ice grain. We obtained the spectral complex RIs of ice from Warren and Brandt (2008) and the spectral complex RIs of dust from Dang et al. (2015). The imaginary part of the complex RIs of ice (k_{ice}) and dust (k_{dust}) associated with absorption is shown in Figure 3. We also evaluated the effect of dust on the imaginary part of the effective complex RIs (k_{ef}) assuming dust mass concentrations (C_{dust}^*) of 1–100 ppm (or µg g^{-1}) in snow.

In all variations of the spatial distribution of dust particles in snow, the dust mass concentration was assumed to be constant, which means that the local dust fraction volume may differ. In an example of spherical ice grains with uniformly distributed dust, the dust fraction volume in an ice grain was determined as:

$$\delta_{dust}^0 = \frac{C_{dust}^*}{C_v} \frac{\rho_{ice}}{\rho_{dust}} \tag{9}$$

where the ratio of C_{dust}^*/C_v is the mass fraction of dust in the ice grain.

We considered two cases of non-uniform dust distributed in a spherical ice grain with radius r_{ef}: (1) We assumed that the same mass of dust is uniformly distributed in the central part of the ice grain ($r_{ef}^{dust} < r_c \leq r_{ef}$). (2) We assumed all of the dust was in the surface layer of the ice grain ($r_{ef}^{dust} < r_p \leq r_{ef}$) (Figure 2). In both cases the local value of δ_{dust} increases as:

$$\delta_{dust} = \delta_{dust}^0 \Big/ \psi \qquad \psi = \begin{cases} \bar{r}_c^3 & \text{central pollution} \\ 1 - (1 - \bar{r}_p)^3 & \text{peripheral pollution} \end{cases} \tag{10}$$

where $\bar{r}_c = r_c/r_{ef}$ and $\bar{r}_p = r_p/r_{ef}$. $\bar{r}_c = 1$ and $\bar{r}_p = 1$ correspond to uniformly distributed dust when $\psi = 1$ and $\delta_{dust} = \delta_{dust}^0$, and $\psi < 1$ and $\delta_{dust} > \delta_{dust}^0$ in other cases. Obviously, dust particles increase the imaginary part of the effective complex RIs in polluted ice grains (Figure 3).

In summary, the m_{ef} of a spherical ice grain with uniformly and non-uniformly distributed , according to Eq. (8) to (10), then their corresponding absorption

efficiencies can be obtained using classical Mie theory and core/shell Mie theory, respectively. The spectral snow albedo for IDM can be easily calculated using Eq. (1) to (5).

2.3 Broadband snow albedo calculations

The spectral albedo (α_λ) is integrated over the solar spectrum ($\lambda = 300–2500$ nm) and weighted by incoming solar irradiance (E_λ) to calculate broadband snow albedo (Hadley and Kirchstetter, 2012):

$$\alpha_{integrated} = \frac{\int \alpha_\lambda E_\lambda d\lambda}{\int E_\lambda d\lambda} \tag{11}$$

Following the study of Dang et al. (2017), the incoming solar irradiance we used is a typical surface solar spectrum at mid to high latitudes from January to March under the cloudy sky, calculated by the Santa Barbara DISORT Atmospheric Radiative Transfer (SBDART) model (Pu et al., 2019). The SBDART model is a widely used atmospheric radiation transfer model based on a collection of highly developed physical models, including the Discrete Ordinate Radiative Transfer module (Stamnes et al., 1988), low-resolution atmospheric transmission models, and Mie theory. The SBDART model can be used to compute radiative transfer at different heights and directions under both clear and cloudy sky conditions. Details on the SBDART model can be found in Ricchiazzi et al. (1998).

2.4 Dust concentration measurements

To estimate the effect of dust on snow albedo in real snowpack, we collected a comprehensive set of in situ dust concentration measurements during field campaigns to Inner Mongolia, China (IMC) (Wang et al., 2013), the Tibetan Plateau (TP) (Li et al., 2017, 2018; Li et al., 2016, 2019; Niu et al., 2017; Qu et al., 2014; Zhang et al., 2017, 2018), Sapporo, Japan (SJ) (Kuchiki et al., 2015), the European Alps (EP) (Di Mauro et al., 2015; Lim et al., 2014), and North American mountains (NAM) (Painter et al., 2012; Reynolds et al., 2020). The field campaigns conducted in the TP can be further grouped into three regions, as in previous $\delta^{18}O$ precipitation studies (Yao et al., 2013).

1 These three distinct domains were associated with the Indian monsoon (Southern TP),

2 westerlies (Northern TP), and transition (Central TP) (Yao et al., 2013). It is worth

3 noting that we only considered regions with higher dust concentrations (>1 ppm), such

4 that polar regions are not included in this study. Measurements of dust in the snow

5 samples were generally obtained by weighing the filter before and after filtration using

6 a microbalance.

7 **3. Results**

8 **3.1 Impact on the imaginary part of the effective complex RIs**

9 We evaluated the effect of dust on k_{ef}, including k_{ice} and k_{dust} associated with absorption

10 (Figure 3). The k_{dust} was in a narrow range (~0.001–0.01) and gradually decreased with

11 increasing wavelength in the ultraviolet (UV) and VIS regions, then remained stable in

12 the NIR band. The k_{ice} varied by eight orders of magnitude from the UV (~10^{-11}) to NIR

13 (~10^{-3}) bands, and increased with increasing wavelength, except at 1.03 μm where k_{ice}

14 decreased slightly as a result of the presence of ice absorption features (Warren, 2019).

15 Figure 3 also shows the k_{ef} with dust mass concentrations ranging from 1 to 100 ppm

16 and wavelengths of 300–1500 nm. The k_{ef} clearly varied depending on the wavelength

17 and increased with dust mass concentrations. For a given dust mass concentration, k_{ef}

18 decreased with wavelengths from UV to VIS, then increased from VIS to NIR. For

19 example, the value of k_{ef} decreased from 4.26×10^{-8} at 300 nm to 1.36×10^{-8} at 500

20 nm, then rose to 1.73×10^{-6} at 1000 nm at a dust concentration of 10 ppm. Moreover,

21 the wavelength of the minimum of k_{ef} varied from ~500 nm to ~650 nm depending on

22 the dust mass concentrations (1 to 100 ppm). Additionally, it is worth noting that k_{ef} was

23 not sensitive to dust mass concentrations in wavelengths >1000 nm, which was

24 generally consistent with k_{ice}, because the difference between k_{dust} and k_{ice} is more than

25 compensated by the much larger difference in ice and dust concentration at those

26 wavelengths. Conversely, k_{ef} showed significant differences relative to k_{ice} in the UV

27 and VIS regions, with higher dust mass concentrations demonstrating larger differences.

1   For example, k_{ef} was enhanced by 3, 21, and 205 times at 500 nm relative to k_{ice} for dust

2   mass concentrations of 1, 10, and 100 ppm, respectively.

3   **3.2 Impact on spectral snow absorption coefficient and albedo**

4   Dust in snow effectively enhances the snow absorption coefficient, but its effect on the

5   snow asymmetry factor and extinction efficiency is negligible (He et al., 2019).

6   Therefore, we mainly focused on the effects of EDM and three cases of IDM (uniform,

7   central, and peripheral) on the snow absorption coefficient (σ_{abs}). Figure 4a displays the

8   σ_{abs} for EDM and IDM (uniform) as a function of wavelength at different dust

9   concentrations. We used a snow grain radius of 200 μm (Figure 4), which is comparable

10   to previous observations of seasonal snow at mid to high latitudes in winter (Shi et al.,

11   2020; Wang et al., 2017). The results showed that EDM and IDM have distinct impacts

12   on σ_{abs} in UV and VIS, but small effects at wavelengths >1000 nm, which is due to

13   the optical properties of snow being affected by LAPs in UV and VIS and primarily

14   affected by snow itself at wavelengths >1000 nm. Additionally, σ_{abs} increased with

15   increased dust mass concentrations. For instance, σ_{abs} increased from 0.007 m^{-1} (pure

16   snow) to 0.03, 0.14, and 1.37 m^{-1} at 500 nm with 2, 10, and 100 ppm of dust with EDM,

17   respectively. For IDM (uniform), σ_{abs} increased to 0.06, 0.28, and 2.80 m^{-1} at 500 nm

18   with 2, 10, and 100 ppm of dust, respectively, with corresponding enhancement factors

19   of σ_{abs} ($E_{\sigma_{abs}}$, defined as the absorption coefficient of IDM divided by EDM) were

20   1.84, 2.00, and 2.05. Furthermore, the σ_{abs} for two cases of non-uniform dust

21   distribution in a spherical ice grain (r_{ef} = 200 μm) depends on the wavelength, dust mass

22   concentrations, $\bar{r}_c$, and $\bar{r}_p$ (Figure 4b and 4c). We note that $\bar{r}_c$ and $\bar{r}_p$ values of 1

23   correspond to uniformly distributed dust, and the σ_{abs} increases and decreases (with

24   the decrease of $\bar{r}_c$ and $\bar{r}_p$) for IDM (central) and IDM (peripheral), respectively. For

25   example, σ_{abs} increased by 29%, 32%, and 33% (500 nm) at dust mass concentrations

26   of 2, 10, and 100 ppm, respectively, when $\bar{r}_c$ decreased from 1 to 0.7 for IDM (central).

27   However, σ_{abs} decreased by 41%, 44%, and 44% (500 nm) at dust mass concentrations

28   of 2, 10, and 100 ppm, respectively, when $\bar{r}_p$ decreased from 1 to 0.1 for IDM

1 (peripheral). This indicates that the IDM (central) further enhanced snowpack light

2 absorption compared with the IDM (uniform), while the IDM (peripheral) reduced

3 snowpack light absorption with a corresponding σ_{abs} between the value of σ_{abs} for

4 IDM (uniform) and EDM. Figure 4d–f quantitatively shows the spectral snow

5 absorption coefficient enhancement for IDM ($E_{\sigma_{abs}}$). The enhancement decreased

6 sharply with increasing wavelengths, then reduced to 1.0 (i.e., no enhancement) at

7 wavelengths longer than ~1.0 μm because of strong dust absorption and weak snow

8 absorption at shorter wavelengths. Obviously, $E_{\sigma_{abs}}$ was affected by dust mass

9 concentration, $\bar{r}_c$, and $\bar{r}_p$, but $E_{\sigma_{abs}}$ was insensitive to dust mass concentration at

10 wavelengths <450 nm.

11 Figure 5a–c shows the spectral snow albedo (α_λ) for EDM and IDM; α_λ was

12 consistent with σ_{abs}, with the effects mainly present at wavelengths <1000 nm.

13 Generally, α_λ decreased with increased dust mass concentrations in UV and VIS, and

14 IDM was shown to further trigger the reduction of α_λ. For example, for EDM α_λ was

15 ~0.97, 0.95, 0.85 (at 500 nm) for dust concentrations of 2, 10, 100 ppm, respectively,

16 which was higher than the values for IDM (uniform) (~0.96, 0.93, 0.79, respectively).

17 Compared with IDM (uniform), the α_λ for IDM (central) decreased by 0.5%, 1.1%,

18 and 3.5% (at 500 nm) for dust concentrations of 2, 10, and 100 ppm, respectively, when

19 $\bar{r}_c$ decreased from 1 to 0.7. α_λ for IDM (peripheral) increased by 0.8%, 1.9%, and 6.2%

20 (at 500 nm) for the same dust concentrations, when $\bar{r}_p$ decreased from 1 to 0.1.

21 Moreover, the wavelength of the maximum α_λ value varied from ~500 nm to ~650 nm

22 depending on the dust mass concentrations, which is consistent with changes of k_{ef}.

23 Figure 5d–f shows the ratio (E_{α_λ}) of snow spectral albedo for IDM to EDM where we

24 observed that the E_{α_λ} increased with increasing wavelengths and dust concentrations,

25 and then became stable at 1.0. This is because IDM can enhance the light absorption of

26 snowpack more effectively at shorter wavelengths and higher dust concentrations

27 (Figure 4). Additionally, the values of $\bar{r}_c$ and $\bar{r}_p$ also have non-negligible effects on

28 E_{α_λ}, which can be decreased and increased with decreasing $\bar{r}_c$ and $\bar{r}_p$, respectively.

1   We found that the optical properties of an ice grain containing uniformly distributed

2   dust in its center, or concentric surface layer, can be affected by $\bar{r}_c$ or $\bar{r}_p$. To better

3   understand this effect, Figure 6a–b displays the σ_{abs} at 500 nm as a function of $\bar{r}_c$ and

4    $\bar{r}_p$ with different dust concentrations and r_{ef}. This demonstrates r_{ef} has negligible

5   effects on σ_{abs} due to the geometric optical limits at $r_{ef} \approx 50$ μm, which shows the

6   universal (independent of r_{ef}) monotonic dependence of σ_{abs} on $\bar{r}_c$ and $\bar{r}_p$ for ice

7   grains with $r_{ef} \geq 50$ μm (Velesco et al., 1997). As a result, the spectral absorption

8   coefficient of snow containing polydispersed ice grains can be obtained using our

9   results for a monodispersed model. Interestingly, σ_{abs} did not depend on $\bar{r}_c$ when $\bar{r}_c$

10   <0.75 and decreased almost linearly at higher $\bar{r}_c$ values (Figure 6a); this phenomenon

11   can be explained by geometric optical effects (Mackowski et al., 1990). However, σ_{abs}

12   was significantly affected by the dust mass concentration; for example, σ_{abs} at 500 nm

13   was decreased by 28%, 32%, and 32% from its maximum value (0.08, 0.38, and 3.71

14   m^{-1}) for dust concentrations of 2, 10, and 100 ppm, respectively, when $\bar{r}_c$ increased

15   from <0.75 to 1.0. The monotonic increase in σ_{abs} with the relative thickness of the

16   polluted ice grain surface layer (i.e., $\bar{r}_p$) was also noteworthy (Figure 6b). The

17   core/shell Mie theory calculations for ice grains with a thin surface layer ($\bar{r}_p = 0.01$)

18   gave almost the same σ_{abs} as that obtained for the EDM. As a result, the σ_{abs}

19   increased rapidly with $\bar{r}_p$ <0.4 and then increased more slowly until $\bar{r}_p = 1$, which

20   corresponds to IDM (uniform).

21   The α_λ at 500 nm as a function of $\bar{r}_c$ and $\bar{r}_p$ with different dust concentrations and

22   r_{ef}, is illustrated in Figure 6c and 6d. In general, α_λ at 500 nm decreased with

23   increasing dust mass concentration and r_{ef}; the effect of grain radius can be explained

24   by the fact that the snow extinction coefficient is inversely proportional to r_{ef}, so that

25   for a given amount of dust, the single-scattering albedo of the snow-dust mixture is

26   smaller for large snow grains (Gardner and Sharp, 2010). For a given dust mass

27   concentration and r_{ef}, the α_λ at 500 nm increased from its minimum value with $\bar{r}_c$

28   <0.75 to the maximum value with $\bar{r}_c = 1$, corresponding to the findings of IDM

1 (uniform). For example, at dust concentrations of 2, 10, and 100 ppm, and a fixed r_{ef} of

2 100 μm, the α_λ at 500 nm increased by 0.~~2~~1%, 0.7%, and ~~0.8~~2.6%, respectively, when

3 $\overline{r_c}$ increased from <0.75 to 1. When the r_{ef} was fixed at 500 μm, the α_λ at 500 nm

4 increased by ~~1.9~~0.8%, ~~2.5~~1.9%, and 6.2% at dust concentrations of 2, 10, and 100 ppm,

5 respectively. Conversely, the α_λ at 500 nm decreased from its maximum value when

6 $\overline{r_p}$ = 0.01 (similar to EDM) to the minimum value with $\overline{r_p}$ = 1, corresponding to the

7 case of IDM (uniform). For example, the α_λ at 500 nm decreased by 0.6%, 1.4%, and

8 ~~1.4~~4.7% when $\overline{r_p}$ increased from 0.01 to 1 for dust concentrations of 2, 10, and 100

9 ppm, respectively, and a fixed r_{ef} of 100 μm, whereas for a r_{ef} of 500 μm, α_λ decreased

10 by ~~3.3~~1.4% (2 ppm dust), ~~4.7~~3.3% (10 ppm), and 10.1% (100 ppm). These results

11 indicate that dust mass concentrations and r_{ef} can amplify the influence of $\overline{r_c}$ or $\overline{r_p}$ on

12 snow albedo. Moreover, the effect of dust mass concentration on snow albedo is similar

13 to r_{ef}. For example, dust mass concentrations of 10 and 100 ppm and r_{ef} of 100 and 50

14 μm gave similar α_λ at 500 nm to dust mass concentrations of 2 and 10 ppm and r_{ef} of

15 500 μm. According to this result, spectral albedo measurements at a single wavelength

16 are insufficient to obtain the mass fraction of dust in snow cover because the same effect

17 can also be explained by a combination of different ice grain sizes and a non-uniform

18 distribution of dust inside the grains. It means that additional information is needed to

19 determine accurate dust mass concentrations. This may be a set of measurements at

20 various wavelengths in the VIS and NIR spectral ranges.

21 **3.3 Effects on broadband snow albedo**

22 Compared with the spectral optical properties, broadband results can provide more

23 general knowledge for the relevant research community. Figure 7 shows the spectrally

24 weighted α_λ ($\alpha_{integrated}$) over 300–2500 nm of a typical surface solar spectrum at mid

25 to high latitudes, which is comparable with previous studies (Dang et al., 2017; Wang

26 et al., 2017). Because the results of IDM (peripheral) effects on snow albedo fell

27 between results from EDM and IDM (central), we do not consider the case of IDM

28 (peripheral) in the following discussion. Instead, we focus on the effects of dust mass

concentration and r_{ef} on broadband snow albedo for EDM and IDM (uniform, central).
Similar to α_λ, $\alpha_{integrated}$ generally decreased with increasing dust mass concentrations and r_{ef} such that $\alpha_{integrated}$ declined more for internal mixing than external mixing. $\alpha_{integrated}$ showed ranges of 0.60–0.92, 0.54–0.92, and 0.51–0.92 for EDM, IDM (uniform), and IDM (central, $\bar{r}_c$ <0.75), respectively, with dust mass concentrations of 0–100 ppm and r_{ef} of 50–1000 μm. For a given dust mass concentration and r_{ef}, $\alpha_{integrated}$ for IDM (uniform) was smaller than EDM, which is due to higher light absorption in the UV and VIS bands for IDM (uniform) relative to EDM (Figure 4a). While $\alpha_{integrated}$ for IDM (uniform) was larger compared with IDM (central, $\bar{r}_c$ <0.75), this can be attributed to the fact that radiation is focused near the center of an ice grain with IDM (central) (Ackerman and Toon, 1981; Bohren, 1986), enabling further absorptions from inclusions near the center of a grain due to the lensing effect (Mackowski et al., 1990). For example, $\alpha_{integrated}$ (dust concentration of 20 ppm, r_{ef} of 500 μm) was 0.73 for IDM (uniform), less than EDM of 0.76, but higher than IDM (central, $\bar{r}_c$ <0.75) of 0.72.

To quantify the effects of IDM on broadband snow albedo relative to EDM, we defined a broadband snow albedo scaling factor ($E_{\alpha,\ integrated}$), which refers to the ratio of $\alpha_{integrated}$ of IDM to EDM. Generally, for dust mass concentrations from 0 to 100 ppm and r_{ef} of 50–1000 μm, $E_{\alpha,\ integrated}$ varied from 0.89 to ~1.00 for IDM (uniform) (Figure 8a) and from 0.85 to ~1.00 for IDM (central, $\bar{r}_c$ <0.75) (Figure 8b). $E_{\alpha,\ integrated}$ decreased significantly with increasing dust mass concentration and r_{ef}. In addition, $E_{\alpha,\ integrated}$ for IDM (central, $\bar{r}_c$ <0.75) was smaller than IDM (uniform). These results have implications for the effects of IDM in real environments. For example, IMC has typical dust concentrations of ~10 ppm (Wang et al., 2013), so $E_{\alpha,\ integrated}$ (r_{ef} of 50–1000 μm) was 0.96–0.99 and 0.95–0.99 for IDM (uniform) and IDM (central, $\bar{r}_c$ < 0.75), respectively. In contrast, dust concentrations are typically ~100 ppm in the TP (Ming et al., 2016; Li et al., 2017, 2018), so $E_{\alpha,\ integrated}$ ranged from 0.89 to 0.98 and 0.85 to 0.96 for IDM (uniform) and IDM (central, $\bar{r}_c$ <0.75), respectively. The results

1 show that IDM (uniform) and IDM (central, $\bar{r}_c$ <0.75) reduced broadband snow

2 albedo by ~2.5% and ~3.0%, respectively, in clean snow and ~6.5% and ~9.5%,

3 respectively, in polluted snow relative to EDM. Moreover, the sensitivity of E$_{\alpha,\ integrated}$

4 to mineral dust decreased with increasing dust concentrations. For example, the

5 difference in E$_{\alpha,\ integrated}$ (r_{ef} of 500 µm) between dust concentrations of 10 and 20 ppm

6 was 0.011 and 0.015 for IDM (uniform) and IDM (central, $\bar{r}_c$ <0.75), respectively,

7 while the corresponding differences between dust concentrations of 90 and 100 ppm

8 were only 0.004 and 0.005. These results provide a convenient method to calculate the

9 albedo of IDM when the albedo of EDM has been obtained for a given dust mass

10 concentration and r_{ef}.

11 **3.4 Uncertainties**

12 Although we calculated the imaginary RI values of dust using previous studies (section

13 2.2), there are still large variations which strongly depend on dust composition (e.g.,

14 hematite/iron content) (Balkanski et al., 2007; Wagner et al., 2012). To roughly account

15 for this, we estimated the influence of chosen imaginary RI values on spectrally

16 weighted snow albedo (E$_{\alpha,\ integrated}$) by increasing and decreasing the calculated

17 imaginary RI values by 50%. These changes in imaginary RIs are plausible because

18 they are consistent with other studies (McConnell et al., 2010; Wagner et al., 2012).

19 The results showed that E$_{\alpha,\ integrated}$ uncertainties attributed to the imaginary RIs of dust

20 were ±3.9% and ±5.2% for IDM (uniform) and IDM (central, $\bar{r}_c$ <0.75), respectively.

21 In contrast, observations have displayed large variations in the size distribution of dust

22 in the atmosphere and snow, and this variation is strongly affected by the dust source

23 and transport (Mahowald et al., 2014; Shao et al., 2011). In our standard simulation, we

24 assumed a log-normal dust size distribution with a geometric mean diameter of 0.65

25 µm and a standard deviation of 2.0 (equivalent to an effective radius of 1.1 µm), which

26 is typical for dust transported long-range (Formenti et al., 2011; Maring et al., 2003);

27 nearer sources of dust tend to be larger (Kok, 2011). Therefore, we investigated the

28 effects of dust particle size on our results by assuming another two log-normal size

1   distributions with effective radii of 2.5 μm and 5.0 μm, which were within the observed

2   size ranges in the atmosphere and snow and comparable with previously analyzed dust

3   particle sizes (Maring et al., 2003; Shao and Mao, 2016; Zhang et al., 2003). The results

4   showed that the uncertainty of $E_{\alpha,\,integrated}$ attributed to dust diameter was ±6.1% for both

5   IDM (uniform) and IDM (central, $\overline{r}_c$ <0.75), but it should be emphasized that this

6   uncertainty estimate accounts only for the impact of dust size on snow albedo in the

7   case of external mixing, since the impact on albedo due to dust size cannot be evaluated

8   when using the effective medium approximation~~the uncertainty of $E_{\alpha,\,integrated}$ induced~~

9   ~~by dust sizes comes purely from the uncertainty of broadband albedo of dust-snow~~

10   ~~external mixing due to different dust sizes.~~ ~~This is because effective complex~~

11   ~~refractive indices of dust-snow internal mixture are independent of dust particle size~~

12   ~~(Eq. 8).~~ Overall, the total uncertainty of $E_{\alpha,\,integrated}$ from variations of imaginary RIs

13   and dust diameter was ±11.0% and ±11.2% for IDM (uniform) and IDM (central, $\overline{r}_c$

14   <0.75), respectively, with dust mass concentrations of 0–100 ppm and r_{ef} of 50–1000

15   μm. Specifically, the uncertainty increased with increasing r_{ef} and dust concentrations.~~.~~

16   **3.5 Measurement-based estimate of the effects of dust on snow albedo**

17   Finally, widespread dust concentrations in snow across the Northern Hemisphere were

18   obtained to assess the effects of dust on snow albedo in real snowpack. Figure 9 shows

19   measured dust concentrations in snow in different regions; dust concentrations spanned

20   a broad range of values because of spatial and temporal variations in emissions,

21   transportation, and deposition among the different regions. Dust concentrations widely

22   varied from ~3 ppm to ~600 ppm, with the highest concentration in NAM and lowest

23   in the EP (Di Mauro et al., 2015; Lim et al., 2014; Painter et al., 2012; Reynolds et al.,

24   2020). However, snow samples collected in the days after a significant dust transport

25   event showed that dust concentrations in snow can be up to ~70 ppm in the EP (Di

26   Mauro et al., 2015). Additionally, the average dust concentrations in fresh snow were

27   18, 6, and 28 ppm in the southern TP, central TP, and northern TP, respectively, similar

28   to the IMC (12 ppm) (Wang et al., 2013). However, dust concentrations in aged snow

1 (120, 300, and 140 ppm) were one to two orders of magnitude higher than in fresh snow,

2 indicating the important correlation between snow type and dust concentration (Zhang

3 et al., 2017, 2018).

4 We calculated the broadband snow albedo for EDM, IDM (uniform), and IDM (central,

5 $\bar{r}_c$ <0.75) based on the measured dust concentrations (Figure 10). The results showed

6 that broadband snow albedo decreased by 0.8%, 1.4%, and 1.6% in the EP for EDM,

7 IDM (uniform), and IDM (central, $\bar{r}_c$ <0.75), respectively, which was similar to SJ.

8 However, the broadband snow albedo decreased by up to 5.6%, 8.1%, and 9.4% in the

9 EP after a significant dust transport event, indicating strong snow albedo reduction

10 during these events. In addition, broadband snow albedo was reduced by 2.0%, 3.1%,

11 and 3.6% in IMC for EDM, IDM (uniform), and IDM (central, $\bar{r}_c$ <0.75), respectively.

12 Similar results were also found for the southern TP, central TP, and northern TP where

13 the broadband snow albedo for fresh snow was reduced by 2.5%, 1.4%, and 3.3%,

14 respectively, for EDM, 3.9%, 2.1%, and 5.1% for IDM (uniform), and 4.5%, 2.4%, and

15 5.7% for IDM (central, $\bar{r}_c$ <0.75). However, the broadband snow albedo was more

16 significantly reduced for aged snow: up to 6.0%, 8.1%, and 7.5% for EDM, 9.5%,

17 11.6%, and 10.5% for IDM (uniform), and 10.9%, 13.2%, and 12.3% for IDM (central,

18 $\bar{r}_c$ <0.75) in the southern, central, and northern TP, respectively. This indicates that the

19 effects of dust on snow albedo showed stronger reductions during snowmelt periods, it

20 is worth noting that the effect of dust on snow albedo for aged snow could be

21 underestimated due to the larger snow grain effective radius (r_{ef}) than fresh snow.

22 Moreover, the largest broadband snow albedo reductions were found in NAM with

23 ranges of 9.8%–17.6%, 13.9%–24.1%, and 15.9%–27.0% for EDM, IDM (uniform),

24 and IDM (central, $\bar{r}_c$ <0.75), respectively. These results suggest that the effects of

25 external or internal dust–snow mixing on snow albedo are particularly significant for

26 the TP and NAM regions, with stronger reductions in albedo. Therefore, these results

27 can have significant impacts on both local hydrological cycles and regional climate

28 change (Oaida et al., 2015; Xie et al., 2018).

4. Discussion

In this study, the application of the effective medium approximation greatly simplifies the complexity of snow radiation transfer calculation for dust–snow internal mixing, and the effect of non-uniform distribution of dust in snow grains on snowpack optical properties are explicitly quantified for the first time. However, it is worth noting that this method has its limitation when applying to large particles (e.g., dust) in snow (Bohren 1986; Flanner et al., 2012), which can create some errors for the albedo calculation of dust–snow internal mixing. To verify the credibility of our results, we carefully make a comparison with the more rigorous calculations found in He et al. (2019), which used the geometric-optics surface-wave approach (GOS) to consider the impact of dust–snow uniform internal mixing on snow albedo reduction. As shown in Figure 11, the results show that the enhancement ratio of snow albedo reduction (1.28) due to dust–snow internal mixing (relative to external mixing) is slightly higher than the value (1.16) reported by He et al. (2019), and this deviation is comparable to that caused by snow nonsphericity (He et al., 2019). Therefore, we indicated that the effective medium approximation used in this study is reasonable and reliable.

Over the past few decades, the effects of dust in snow on reductions in albedo have been widely demonstrated (Skiles et al., 2018; Zhang et al., 2018). However, the magnitude of these effects has only been studied in a few regions, and uncertainties still remain. Our study indicates that the albedo of dust-contaminated snowpack can be affected by the dust–ice mixing state. In particular, IDM enhanced light absorption and reduced snow albedo more significantly compared with EDM. For example, in IMC and the TP, IDM reduced snow albedo by ~5% relative to EDM at a typical dust mass concentration of 20 ppm and a snow grain radius of 500 μm. This exceeds the contribution of BC to snow light absorption over most areas of North America and the Arctic (Dang et al., 2017). In addition, the effects of IDM on snow albedo were amplified by higher dust mass concentrations and larger snow grain sizes. We therefore strongly suggest that IDM must be considered in future climate models, particularly to

1   more accurately evaluate the climate in areas where snowpack is heavily contaminated

2   with dust and is experiencing melting.

3   The mixed state between dust and snow gradually progresses from partial external

4   mixing to wholly internally mixed. Therefore, assuming a completely external mixing

5   of dust and snow grains will underestimate the effects of dust on snow albedo and

6   radiative forcing in numerical models (e.g., Dang et al., 2015; Nagorski et al., 2019).

7   Similarly, assuming completely internal mixing of dust and snow grains will

8   overestimate the effects of dust (e.g., He et al., 2019; Liou et al., 2014). Zhao et al.

9   (2014) underestimated the effects of dust by treating wet-deposited dust as externally

10 mixed with snow grains. In future studies, we recommend the actual ratio between

11 external and internal mixing for dust in snow be examined with an environmental

12 scanning electron microscope equipped with a cold stage.

13 **5. Conclusions**

14 In this study, the effects of dust particles on absorption coefficients and snow albedo

15 were theoretically analyzed by combining asymptotic radiative transfer theory and

16 (core/shell) Mie theory. We initially considered external mixing – when dust is present

17 between ice grains – and variations of internal mixing of dust within ice grains. We

18 found that snow spectral absorption coefficients of IDM were larger than EDM across

19 UV to NIR wavelengths, but were negligible at wavelengths >1000 nm. The absorption

20 enhancement (relative to EDM) was wavelength-dependent and increased with

21 increased dust concentrations.

22 Compared with a uniform distribution of dust particles in ice grains, our calculations

23 showed that non-uniformly distributed dust particles may lead to significantly different

24 snow spectral absorption coefficients in the VIS band. Snow spectral absorption

25 coefficients were further increased when all of the dust was positioned in the central

26 part of ice grains, while the maximum absorption coefficient was found when the radius

27 of a dust-polluted core was <75% of the ice grain radius. In contrast, snow spectral

28 absorption coefficients decreased when all of the dust was positioned in the surface

layer of ice grains, and the minimum absorption coefficient was observed in the thin surface layer of dust-polluted ice grains, which was similar for EDM. As a result, broadband snow albedo decreased by up to 21%, 30%, and 33% for EDM, IDM (uniform), and IDM (central, $\bar{r}_c < 0.75$), respectively, at dust concentrations of 100 ppm and r_{ef} of 1000 μm.

Based on comprehensive field measurements across the Northern Hemisphere, the effect of dust on snow albedo in real snowpack was evaluated by assuming external and internal dust–snow mixing. The largest reductions in broadband snow albedo were in NAM because that region had the highest average dust concentrations; IDM (uniform) and IDM (central, $\bar{r}_c < 0.75$) further decreased snow albedo by 4.6%–7.8% and 6.8%–11.4%, respectively, compared with EDM. This implies an important influence of internal dust–snow mixing in NAM.

Data availability

The code of (core/shell) Mie theory used in this study can be found at http://gwest.gats-inc.com/software/software_page.html.

Author contributions

WX designed the study and evolved the overarching research goals and aims. STL wrote the first draft with contributions from all co-authors. STL and CJC applied formal techniques such as statistical, mathematical, and computational to analyze study data. CY and XXY collected the dust measurements across the Northern Hemisphere. ZY and PW provided the majority of the methodology and software. CQL and ZXL provided technical guidance. All authors contributed to the improvement of results and revised the final paper.

Competing interests

The authors declare that they have no conflict of interest.

Acknowledgments

1   This work was supported by the National Science Fund for Distinguished Young

2   Scholars (42025102), the National Key Research and Development Program of China

3   (grant number 2019YFA0606801), and the National Natural Science Foundation of

4   China (grant number 41975157, 41775144 and 42075061).

References

Aoki, T., Aoki, T., Fukabori, M., Hachikubo, A., Tachibana, Y., and Nishio, F.: Effects of snow physical parameters on spectral albedo and bidirectional reflectance of snow surface, J Geophys Res-Atmos, 105, 10219-10236, 10.1029/1999jd901122, 2000.

Balkanski, Y., Schulz, M., Claquin, T., and Guibert, S.: Reevaluation of Mineral aerosol radiative forcings suggests a better agreement with satellite and AERONET data, Atmos. Chem. Phys., 7, 81-95, 10.5194/acp-7-81-2007, 2007.

Bohren, C. F.: Applicability of Effective-Medium Theories to Problems of Scattering and Absorption by Nonhomogeneous Atmospheric Particles, J Atmos Sci, 43, 468-475, 10.1175/1520-0469(1986)043<0468:Aoemtt>2.0.Co;2, 1986.

Casey, K. A., Kaspari, S. D., Skiles, S. M., Kreutz, K., and Handley, M. J.: The spectral and chemical measurement of pollutants on snow near South Pole, Antarctica, J Geophys Res-Atmos, 122, 6592-6610, 10.1002/2016jd026418, 2017.

Creamean, J. M., Suski, K. J., Rosenfeld, D., Cazorla, A., DeMott, P. J., Sullivan, R. C., White, A. B., Ralph, F. M., Minnis, P., Comstock, J. M., Tomlinson, J. M., and Prather, K. A.: Dust and Biological Aerosols from the Sahara and Asia Influence Precipitation in the Western U.S., Science, 339, 1572-1578, 10.1126/science.1227279, 2013.

Dang, C., Brandt, R. E., and Warren, S. G.: Parameterizations for narrowband and broadband albedo of pure snow and snow containing mineral dust and black carbon, J Geophys Res-Atmos, 120, 5446-5468, 10.1002/2014JD022646, 2015.

Dang, C., Fu, Q., and Warren, S. G.: Effect of Snow Grain Shape on Snow Albedo, J Atmos Sci, 73, 3573-3583, 10.1175/JAS-D-15-0276.1, 2016.

Dang, C., Warren, S. G., Fu, Q., Doherty, S. J., Sturm, M., and Su, J.: Measurements of light-absorbing particles in snow across the Arctic, North America, and China: Effects on surface albedo, J Geophys Res-Atmos, 122, 10149-10168, 10.1002/2017jd027070, 2017.

DeMott, P. J., Prenni, A. J., Liu, X., Kreidenweis, S. M., Petters, M. D., Twohy, C. H., Richardson, M. S., Eidhammer, T., and Rogers, D. C.: Predicting global atmospheric

ice nuclei distributions and their impacts on climate, P Natl Acad Sci USA, 107, 11217-11222, 10.1073/pnas.0910818107, 2010.

Di Mauro, B., Fava, F., Ferrero, L., Garzonio, R., Baccolo, G., Delmonte, B., and Colombo, R.: Mineral dust impact on snow radiative properties in the European Alps combining ground, UAV, and satellite observations, J Geophys Res-Atmos, 120, 6080-6097, 10.1002/2015jd023287, 2015.

Di Mauro, B., Garzonio, R., Baccolo, G., Franzetti, A., Pittino, F., Leoni, B., Remias, D., Colombo, R., and Rossini, M.: Glacier algae foster ice-albedo feedback in the European Alps, Sci Rep-Uk, 10, 4739, 10.1038/s41598-020-61762-0, 2020.

Dombrovsky L. A., and Baillis D.: Thermal radiation in disperse systems: an engineering approach. New York: Begell House, 2010.

Dombrovsky, L. A., and Kokhanovsky, A. A.: Light absorption by polluted snow cover: Internal versus external mixture of soot, Journal of Quantitative Spectroscopy and Radiative Transfer, 242, 106799, 10.1016/j.jqsrt.2019.106799, 2020.

Flanner, M. G., Zender, C. S., Randerson, J. T., and Rasch, P. J.: Present-day climate forcing and response from black carbon in snow, Journal of Geophysical Research, 112, 10.1029/2006jd008003, 2007.

Flanner, M. G., Shell, K. M., Barlage, M., Perovich, D. K., and Tschudi, M. A.: Radiative forcing and albedo feedback from the Northern Hemisphere cryosphere between 1979 and 2008, Nat Geosci, 4, 151-155, 10.1038/ngeo1062, 2011.

Flanner, M. G., Liu, X., Zhou, C., Penner, J. E., and Jiao, C.: Enhanced solar energy absorption by internally-mixed black carbon in snow grains, Atmos Chem Phys, 12, 4699-4721, 10.5194/acp-12-4699-2012, 2012.

Formenti, P., Schutz, L., Balkanski, Y., Desboeufs, K., Ebert, M., Kandler, K., Petzold, A., Scheuvens, D., Weinbruch, S., and Zhang, D.: Recent progress in understanding physical and chemical properties of African and Asian mineral dust, Atmos Chem Phys, 11, 8231-8256, 10.5194/acp-11-8231-2011, 2011.

France, J. L., Reay, H. J., King, M. D., Voisin, D., Jacobi, H. W., Domine, F., Beine, H.,

Anastasio, C., MacArthur, A., and Lee-Taylor, J.: Hydroxyl radical and NOx production rates, black carbon concentrations and light-absorbing impurities in snow from field measurements of light penetration and nadir reflectivity of onshore and offshore coastal Alaskan snow, J Geophys Res-Atmos, 117, 10.1029/2011jd016639, 2012.

Gabbi, J., Huss, M., Bauder, A., Cao, F., and Schwikowski, M.: The impact of Saharan dust and black carbon on albedo and long-term mass balance of an Alpine glacier, Cryosphere, 9, 1385-1400, 10.5194/tc-9-1385-2015, 2015.

Gardner, A. S., and Sharp, M. J.: A review of snow and ice albedo and the development of a new physically based broadband albedo parameterization, Journal of Geophysical Research, 115, 10.1029/2009jf001444, 2010.

Grenfell, T. C., Light, B., and Sturm, M.: Spatial distribution and radiative effects of soot in the snow and sea ice during the SHEBA experiment, J Geophys Res-Oceans, 107, 10.1029/2000jc000414, 2002.

Hadley, O. L., and Kirchstetter, T. W.: Black-carbon reduction of snow albedo, Nat Clim Change, 2, 437-440, 10.1038/nclimate1433, 2012.

Hansen, J., and Nazarenko, L.: Soot climate forcing via snow and ice albedos, P Natl Acad Sci USA, 101, 423-428, 10.1073/pnas.2237157100, 2004.

He, C., Liou, K.-N., Takano, Y., Chen, F., and Barlage, M.: Enhanced Snow Absorption and Albedo Reduction by Dust-Snow Internal Mixing: Modeling and Parameterization, J Adv Model Earth Sy, n/a, 10.1029/2019ms001737, 2019.

He, C. L., Flanner, M. G., Chen, F., Barlage, M., Liou, K. N., Kang, S. C., Ming, J., and Qian, Y.: Black carbon-induced snow albedo reduction over the Tibetan Plateau: uncertainties from snow grain shape and aerosol-snow mixing state based on an updated SNICAR model, Atmos Chem Phys, 18, 11507-11527, 10.5194/acp-18-11507-2018, 2018.

Horhold, M. W., Laepple, T., Freitag, J., Bigler, M., Fischer, H., and Kipfstuhl, S.: On the impact of impurities on the densification of polar firn, Earth Planet Sc Lett, 325, 93-99, 10.1016/j.epsl.2011.12.022, 2012.

Huang, J. P., Wang, T. H., Wang, W. C., Li, Z. Q., and Yan, H. R.: Climate effects of dust aerosols over East Asian arid and semiarid regions, J Geophys Res-Atmos, 119, 11398-11416, 10.1002/2014JD021796, 2014.

Jacobson, M. Z.: Climate response of fossil fuel and biofuel soot, accounting for soot's feedback to snow and sea ice albedo and emissivity, J Geophys Res-Atmos, 109, 10.1029/2004jd004945, 2004.

Kaspari, S., Skiles, S. M., Delaney, I., Dixon, D., and Painter, T. H.: Accelerated glacier melt on Snow Dome, Mount Olympus, Washington, USA, due to deposition of black carbon and mineral dust from wildfire, J Geophys Res-Atmos, 120, 2793-2807, 10.1002/2014jd022676, 2015.

Kok, J. F.: A scaling theory for the size distribution of emitted dust aerosols suggests climate models underestimate the size of the global dust cycle, P Natl Acad Sci USA, 108, 1016-1021, 10.1073/pnas.1014798108, 2011.

Kokhanovsky, A.: Spectral reflectance of solar light from dirty snow: a simple theoretical model and its validation, Cryosphere, 7, 1325-1331, 10.5194/tc-7-1325-2013, 2013.

Kokhanovsky, A. A., and Zege, E. P.: Scattering optics of snow, Appl Optics, 43, 1589-1602, 10.1364/AO.43.001589, 2004.

Koledintseva, M. Y., DuBroff, R. E., and Schwartz, R. W.: Maxwell Garnett Rule for Dielectric Mixtures with Statistically Distributed Orientations of Inclusions, Prog Electromagn Res, 99, 131-148, 10.2528/PIER09091605, 2009.

Kuchiki, K., Aoki, T., Niwano, M., Matoba, S., Kodama, Y., and Adachi, K.: Elemental carbon, organic carbon, and dust concentrations in snow measured with thermal optical and gravimetric methods: Variations during the 2007-2013 winters at Sapporo, Japan, J Geophys Res-Atmos, 120, 868-882, 10.1002/2014JD022144, 2015.

Li, X. F., Kang, S. C., He, X. B., Qu, B., Tripathee, L., Jing, Z. F., Paudyal, R., Li, Y., Zhang, Y. L., Yan, F. P., Li, G., and Li, C. L.: Light-absorbing impurities accelerate glacier melt in the Central Tibetan Plateau, Sci Total Environ, 587, 482-490,

10.1016/j.scitotenv.2017.02.169, 2017.

Li, X. F., Kang, S. C., Zhang, G. S., Qu, B., Tripathee, L., Paudyal, R., Jing, Z. F., Zhang, Y. L., Yan, F. P., Li, G., Cui, X. Q., Xu, R., Hu, Z. F., and Li, C. L.: Light-absorbing impurities in a southern Tibetan Plateau glacier: Variations and potential impact on snow albedo and radiative forcing, Atmos Res, 200, 77-87, 10.1016/j.atmosres.2017.10.002, 2018.

Li, Y., Chen, J., Kang, S., Li, C., Qu, B., Tripathee, L., Yan, F., Zhang, Y., Guo, J., Gul, C., and Qin, X.: Impacts of black carbon and mineral dust on radiative forcing and glacier melting during summer in the Qilian Mountains, northeastern Tibetan Plateau, The Cryosphere Discuss., 2016, 1-14, 10.5194/tc-2016-32, 2016.

Li, Y., Kang, S., Chen, J., Hu, Z., Wang, K., Paudyal, R., Liu, J., Wang, X., Qin, X., and Sillanpää, M.: Black carbon in a glacier and snow cover on the northeastern Tibetan Plateau: Concentrations, radiative forcing and potential source from local topsoil, Sci Total Environ, 10.1016/j.scitotenv.2019.05.469, 2019.

Libois, Q., Picard, G., France, J. L., Arnaud, L., Dumont, M., Carmagnola, C. M., and King, M. D.: Influence of grain shape on light penetration in snow, Cryosphere, 7, 1803-1818, 10.5194/tc-7-1803-2013, 2013.

Lim, S., Fain, X., Zanatta, M., Cozic, J., Jaffrezo, J. L., Ginot, P., and Laj, P.: Refractory black carbon mass concentrations in snow and ice: method evaluation and inter-comparison with elemental carbon measurement, Atmospheric Measurement Techniques, 7, 3307-3324, 10.5194/amt-7-3307-2014, 2014.

Liou, K. N., Takano, Y., and Yang, P.: Light absorption and scattering by aggregates: Application to black carbon and snow grains, J Quant Spectrosc Ra, 112, 1581-1594, 10.1016/j.jqsrt.2011.03.007, 2011.

Liou, K. N., Takano, Y., He, C., Yang, P., Leung, L. R., Gu, Y., and Lee, W. L.: Stochastic parameterization for light absorption by internally mixed BC/dust in snow grains for application to climate models, J Geophys Res-Atmos, 119, 7616-7632, 10.1002/2014jd021665, 2014.

Mackowski, D. W., Altenkirch, R. A., and Menguc, M. P.: Internal Absorption Cross-Sections in a Stratified Sphere, Appl Optics, 29, 1551-1559, 10.1364/AO.29.001551, 1990.

Mahowald, N., Albani, S., Kok, J. F., Engelstaeder, S., Scanza, R., Ward, D. S., and Flanner, M. G.: The size distribution of desert dust aerosols and its impact on the Earth system, Aeolian Res, 15, 53-71, 10.1016/j.aeolia.2013.09.002, 2014.

Maring, H., Savoie, D. L., Izaguirre, M. A., Custals, L., and Reid, J. S.: Mineral dust aerosol size distribution change during atmospheric transport, J Geophys Res-Atmos, 108, 10.1029/2002JD002536, 2003.

Markel, V. A.: Introduction to the Maxwell Garnett approximation: tutorial, J Opt Soc Am A, 33, 1244-1256, 10.1364/JOSAA.33.001244, 2016.

Marley, N. A., Gaffney, J. S., Baird, C., Blazer, C. A., Drayton, P. J., and Frederick, J. E.: An empirical method for the determination of the complex refractive index of size-fractionated atmospheric aerosols for radiative transfer calculations, Aerosol Sci Tech, 34, 535-549, 10.1080/02786820118599, 2001.

Matt, F. N., Burkhart, J. F., and Pietikäinen, J. P.: Modelling hydrologic impacts of light absorbing aerosol deposition on snow at the catchment scale, Hydrol. Earth Syst. Sci., 22, 179-201, 10.5194/hess-22-179-2018, 2018.

Maxwell-Garnett, J. C., and Larmor, J.: XII. Colours in metal glasses and in metallic films, Philosophical Transactions of the Royal Society of London. Series A, Containing Papers of a Mathematical or Physical Character, 203, 385-420, 10.1098/rsta.1904.0024, 1904.

McConnell, C. L., Formenti, P., Highwood, E. J., and Harrison, M. A. J.: Using aircraft measurements to determine the refractive index of Saharan dust during the DODO Experiments, Atmos Chem Phys, 10, 3081-3098, 10.5194/acp-10-3081-2010, 2010.

Ming, J., Xiao, C. D., Wang, F. T., Li, Z. Q., and Li, Y. M.: Grey Tienshan Urumqi Glacier No.1 and light-absorbing impurities, Environ Sci Pollut R, 23, 9549-9558, 10.1007/s11356-016-6182-7, 2016.

Nagorski, S. A., Kaspari, S. D., Hood, E., Fellman, J. B., and Skiles, S. M. J. J. o. G. R. A.: Radiative Forcing by Dust and Black Carbon on the Juneau Icefield, Alaska, 10.1029/2018JD029411, 2019.

Niu, H. W., Kang, S. C., Zhang, Y. L., Shi, X. Y., Shi, X. F., Wang, S. J., Li, G., Yan, X. G., Pu, T., and He, Y. Q.: Distribution of light-absorbing impurities in snow of glacier on Mt. Yulong, southeastern Tibetan Plateau, Atmos Res, 197, 474-484, 10.1016/j.atmosres.2017.07.004, 2017.

Niwano, M., Aoki, T., Kuchiki, K., Hosaka, M., and Kodama, Y.: Snow Metamorphism and Albedo Process (SMAP) model for climate studies: Model validation using meteorological and snow impurity data measured at Sapporo, Japan, J Geophys Res-Earth, 117, -, 10.1029/2011jf002239, 2012.

Oaida, C. M., Xue, Y. K., Flanner, M. G., Skiles, S. M., De Sales, F., and Painter, T. H.: Improving snow albedo processes in WRF/SSiB regional climate model to assess impact of dust and black carbon in snow on surface energy balance and hydrology over western US, J Geophys Res-Atmos, 120, 3228-3248, 10.1002/2014JD022444, 2015.

Painter, T. H., Skiles, S. M., Deems, J. S., Bryant, A. C., and Landry, C. C.: Dust radiative forcing in snow of the Upper Colorado River Basin: 1. A 6 year record of energy balance, radiation, and dust concentrations, Water Resour Res, 48, 10.1029/2012WR011985, 2012.

Pu, W., Cui, J., Shi, T., Zhang, X., He, C., and Wang, X.: The remote sensing of radiative forcing by light-absorbing particles (LAPs) in seasonal snow over northeastern China, Atmos. Chem. Phys., 19, 9949-9968, 10.5194/acp-19-9949-2019, 2019.

Qian, Y., Yasunari, T. J., Doherty, S. J., Flanner, M. G., Lau, W. K. M., Ming, J., Wang, H. L., Wang, M., Warren, S. G., and Zhang, R. D.: Light-absorbing Particles in Snow and Ice: Measurement and Modeling of Climatic and Hydrological impact, Advances in Atmospheric Sciences, 32, 64-91, 10.1007/s00376-014-0010-0, 2015.

Qu, B., Ming, J., Kang, S. C., Zhang, G. S., Li, Y. W., Li, C. D., Zhao, S. Y., Ji, Z. M., and Cao, J. J.: The decreasing albedo of the Zhadang glacier on western

Nyainqentanglha and the role of light-absorbing impurities, Atmos Chem Phys, 14, 11117-11128, 10.5194/acp-14-11117-2014, 2014.

Rahimi, S., Liu, X., Wu, C., Lau, W. K., Brown, H., Wu, M., and Qian, Y.: Quantifying snow darkening and atmospheric radiative effects of black carbon and dust on the South Asian monsoon and hydrological cycle: experiments using variable-resolution CESM, Atmos. Chem. Phys., 19, 12025-12049, 10.5194/acp-19-12025-2019, 2019.

Rango, A., Wergin, W. P., and Erbe, E. F.: Snow crystal imaging using scanning electron microscopy .2. Metamorphosed snow, Hydrolog Sci J, 41, 235-250, 10.1080/02626669609491495, 1996.

Reay, H. J., France, J. L., and King, M. D.: Decreased albedo, e-folding depth and photolytic OH radical and NO2 production with increasing black carbon content in Arctic snow, J Geophys Res-Atmos, 117, 10.1029/2011jd016630, 2012.

Reynolds, R. L., Goldstein, H. L., Moskowitz, B. M., Kokaly, R. F., Munson, S. M., Solheid, P., Breit, G. N., Lawrence, C. R., and Derry, J.: Dust deposited on snow cover in the San Juan Mountains, Colorado, 2011-2016: Compositional variability bearing on snow-melt effects, Journal of Geophysical Research: Atmospheres, n/a, e2019JD032210, 10.1029/2019JD032210, 2020.

Ricchiazzi, P., Yang, S. R., Gautier, C., and Sowle, D.: SBDART: A research and teaching software tool for plane-parallell radiative transfer in the Earth's atmosphere, Bulletin of the American Meteorological Society, 79, 2101-2114, 10.1175/1520-0477(1998)079<2101:Sarats>2.0.Co;2, 1998.

Shao, J. F., and Mao, J. D.: Dust Particle Size Distributions during Spring in Yinchuan, China, Adv Meteorol, 2016, 10.1155/2016/6940502, 2016.

Shao, Y. P., Wyrwoll, K. H., Chappell, A., Huang, J. P., Lin, Z. H., McTainsh, G. H., Mikami, M., Tanaka, T. Y., Wang, X. L., and Yoon, S.: Dust cycle: An emerging core theme in Earth system science, Aeolian Res, 2, 181-204, 10.1016/j.aeolia.2011.02.001, 2011.

Shi, T., Pu, W., Zhou, Y., Cui, J., Zhang, D., and Wang, X.: Albedo of Black Carbon-

Contaminated Snow Across Northwestern China and the Validation With Model Simulation, Journal of Geophysical Research: Atmospheres, 125, e2019JD032065, 10.1029/2019JD032065, 2020.

Skiles, S. M., Flanner, M., Cook, J. M., Dumont, M., and Painter, T. H.: Radiative forcing by light-absorbing particles in snow, Nat Clim Change, 1, 10.1038/s41558-018-0296-5, 2018.

Spaulding, N. E., Meese, D. A., and Baker, I.: Advanced microstructural characterization of four East Antarctic firn/ice cores, J Glaciol, 57, 796-810, 10.3189/002214311798043807, 2011.

Stamnes, K., Tsay, S. C., Wiscombe, W., and Jayaweera, K.: Numerically Stable Algorithm for Discrete-Ordinate-Method Radiative-Transfer in Multiple-Scattering and Emitting Layered Media, Appl Optics, 27, 2502-2509, 10.1364/Ao.27.002502, 1988.

Usha, K. H., Nair, V. S., and Babu, S. S.: Modeling of aerosol induced snow albedo feedbacks over the Himalayas and its implications on regional climate, Climate Dynamics, 10.1007/s00382-020-05222-5, 2020.

Velesco, N., Kaiser, T., and Schweiger, G.: Computation of the internal field of a large spherical particle by use of the geometrical-optics approximation, Appl Optics, 36, 8724-8728, 10.1364/AO.36.008724, 1997.

Wagner, R., Ajtai, T., Kandler, K., Lieke, K., Linke, C., Müller, T., Schnaiter, M., and Vragel, M.: Complex refractive indices of Saharan dust samples at visible and near UV wavelengths: a laboratory study, Atmos. Chem. Phys., 12, 2491-2512, 10.5194/acp-12-2491-2012, 2012.

Wang, X., Doherty, S. J., and Huang, J.: Black carbon and other light-absorbing impurities in snow across Northern China, Journal of Geophysical Research: Atmospheres, 118, 1471-1492, 10.1029/2012jd018291, 2013.

Wang, X., Pu, W., Ren, Y., Zhang, X., Zhang, X., Shi, J., Jin, H., Dai, M., and Chen, Q.: Observations and model simulations of snow albedo reduction in seasonal snow due to

insoluble light-absorbing particles during 2014 Chinese survey, Atmos Chem Phys, 17, 2279-2296, 10.5194/acp-17-2279-2017, 2017.

Warren, S. G., and Wiscombe, W. J.: A Model for the Spectral Albedo of Snow .2. Snow Containing Atmospheric Aerosols, J Atmos Sci, 37, 2734-2745, 10.1175/1520-0469(1980)037<2734:Amftsa>2.0.Co;2, 1980.

Warren, S. G.: Impurities in Snow - Effects on Albedo and Snowmelt Review, Ann Glaciol, 5, 177-179, 10.3189/1984AoG5-1-177-179, 1984.

Warren, S. G., Brandt, R. E., and Grenfell, T. C.: Visible and near-ultraviolet absorption spectrum of ice from transmission of solar radiation into snow, Appl Optics, 45, 5320-5334, 10.1364/Ao.45.005320, 2006.

Warren, S. G., and Brandt, R. E.: Optical constants of ice from the ultraviolet to the microwave: A revised compilation, J Geophys Res-Atmos, 113, 10.1029/2007JD009744, 2008.

Warren, S. G.: Optical properties of ice and snow, Philos T R Soc A, 377, 10.1098/rsta.2018.0161, 2019.

Xie, X. N., Liu, X. D., Che, H. Z., Xie, X. X., Li, X. Z., Shi, Z. G., Wang, H. L., Zhao, T. L., and Liu, Y. G.: Radiative feedbacks of dust in snow over eastern Asia in CAM4-BAM, Atmos Chem Phys, 18, 12683-12698, 10.5194/acp-18-12683-2018, 2018.

Yao, T. D., Masson-Delmotte, V., Gao, J., Yu, W. S., Yang, X. X., Risi, C., Sturm, C., Werner, M., Zhao, H. B., He, Y., Ren, W., Tian, L. D., Shi, C. M., and Hou, S. G.: A review of climatic controls on $\delta^{18}O$ in precipitation over the Tibetan Plateau: Observations and simulations, Reviews of Geophysics, 51, 10.1002/rog.20023, 2013.

Yasunari, T. J., Koster, R. D., Lau, K. M., Aoki, T., Sud, Y. C., Yamazaki, T., Motoyoshi, H., and Kodama, Y.: Influence of dust and black carbon on the snow albedo in the NASA Goddard Earth Observing System version 5 land surface model, J Geophys Res-Atmos, 117, 10.1029/2012jd018691, 2012.

Yasunari, T. J., Koster, R. D., Lau, W. K. M., and Kim, K. M.: Impact of snow darkening via dust, black carbon, and organic carbon on boreal spring climate in the Earth system,

J Geophys Res-Atmos, 120, 5485-5503, 10.1002/2014jd022977, 2015.

Zege, E. P., Ivanov, A. P., and Katsev, I. L.: Image transfer through a scattering medium. Berlin, Springer-Verlag, 1991.

Zender, C. S., Bian, H. S., and Newman, D.: Mineral Dust Entrainment and Deposition (DEAD) model: Description and 1990s dust climatology, J Geophys Res-Atmos, 108, 10.1029/2002JD002775, 2003.

Zhang, D., Iwasaka, Y., Shi, G., Zang, J., Matsuki, A., and Trochkine, D.: Mixture state and size of Asian dust particles collected at southwestern Japan in spring 2000, Journal of Geophysical Research: Atmospheres, 108, 10.1029/2003JD003869, 2003.

Zhang, Y. L., Kang, S. C., Cong, Z. Y., Schmale, J., Sprenger, M., Li, C. L., Yang, W., Gao, T. G., Sillanpaa, M., Li, X. F., Liu, Y. J., Chen, P. F., and Zhang, X. L.: Light-absorbing impurities enhance glacier albedo reduction in the southeastern Tibetan plateau, J Geophys Res-Atmos, 122, 6915-6933, 10.1002/2016jd026397, 2017.

Zhang, Y. L., Kang, S. C., Sprenger, M., Cong, Z. Y., Gao, T. G., Li, C. L., Tao, S., Li, X. F., Zhong, X. Y., Xu, M., Meng, W. J., Neupane, B., Qin, X., and Sillanpaa, M.: Black carbon and mineral dust in snow cover on the Tibetan Plateau, Cryosphere, 12, 413-431, 10.5194/tc-12-413-2018, 2018.

Zhao, C., Hu, Z., Qian, Y., Leung, L. R., Huang, J., Huang, M., Jin, J., Flanner, M. G., Zhang, R., Wang, H., Yan, H., Lu, Z., and Streets, D. G.: Simulating black carbon and dust and their radiative forcing in seasonal snow: a case study over North China with field campaign measurements, Atmos Chem Phys, 14, 11475-11491, 10.5194/acp-14-11475-2014, 2014.

Zhou, X. B., Li, S. S., and Stamnes, K.: Effects of vertical inhomogeneity on snow spectral albedo and its implication for optical remote sensing of snow, J Geophys Res-Atmos, 108, 10.1029/2003JD003859, 2003.
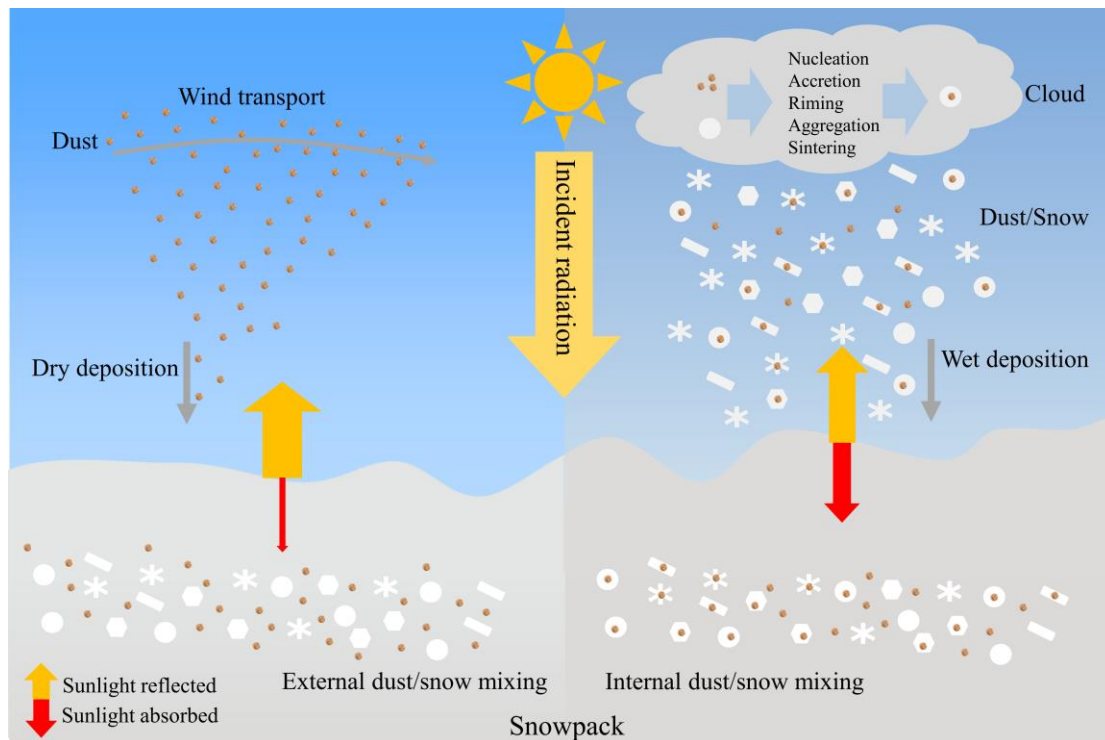
2 **Figure 1.** Schematic of dust mixing with snow grains internally. Dust tends to mix
3 externally with snow grains through dry deposition and/or below cloud scavenging,
4 while dust–snow internal mixtures can be produced by nucleation, accretion, riming,
5 aggregation, and sintering during aerosol–cloud–precipitation processes known as wet
6 deposition. Arrows represent how the absorption (red) and reflection (yellow) of
7 incoming sunlight changes with dust–snow mixing state.

External dust/ice mixing (EDM)
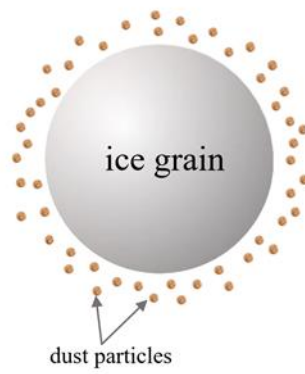
Internal dust/ice mixing (IDM)
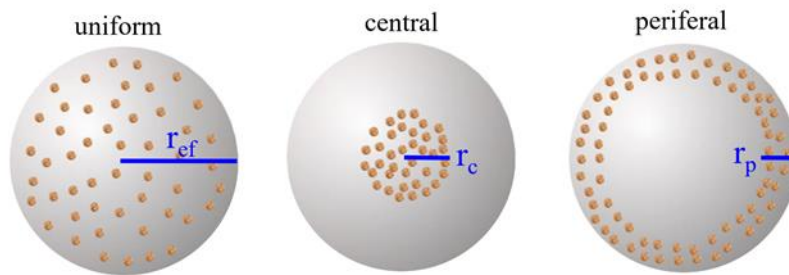
2 **Figure 2.** Schematic depicting various mixing scenarios of snow grains and dust
3 particles.
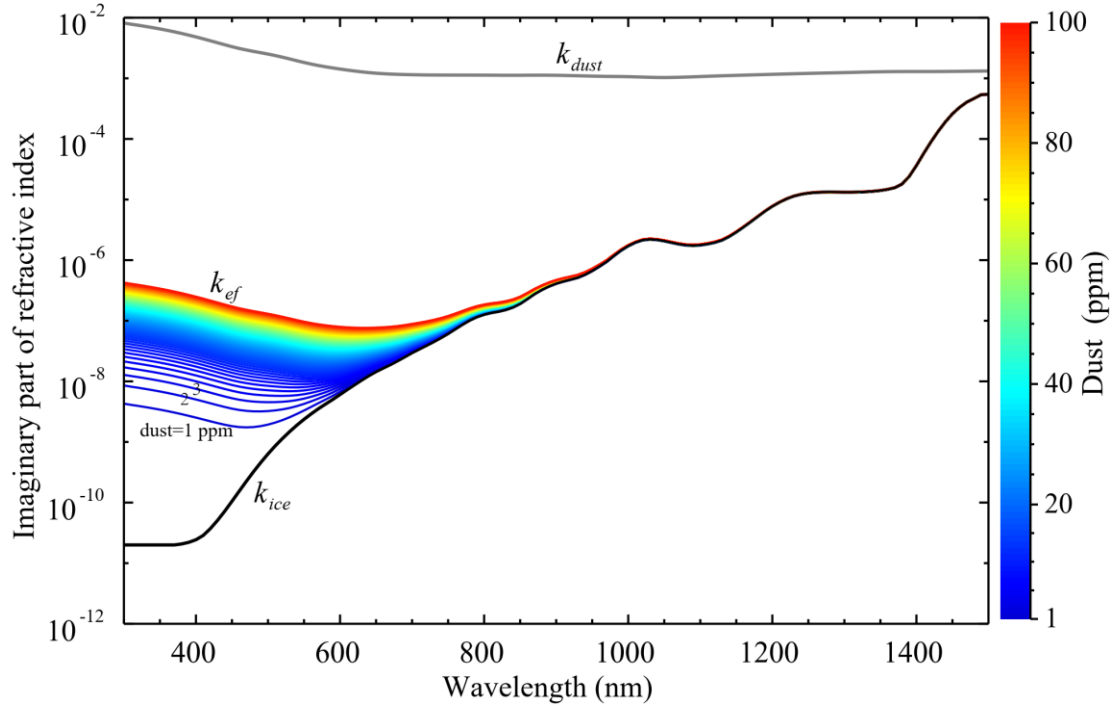
2 **Figure 3.** Imaginary part of the spectral complex refractive indices of ice (k_{ice}) and dust
3 (k_{dust}) (Warren and Brandt, 2008; Dang et al., 2015), with the imaginary part of the
4 effective complex refractive indices (k_{ef}) as a function of wavelength, at dust mass
5 concentrations (C_{dust}^*) of 1–100 ppm (or µg g^{-1}) in snow.
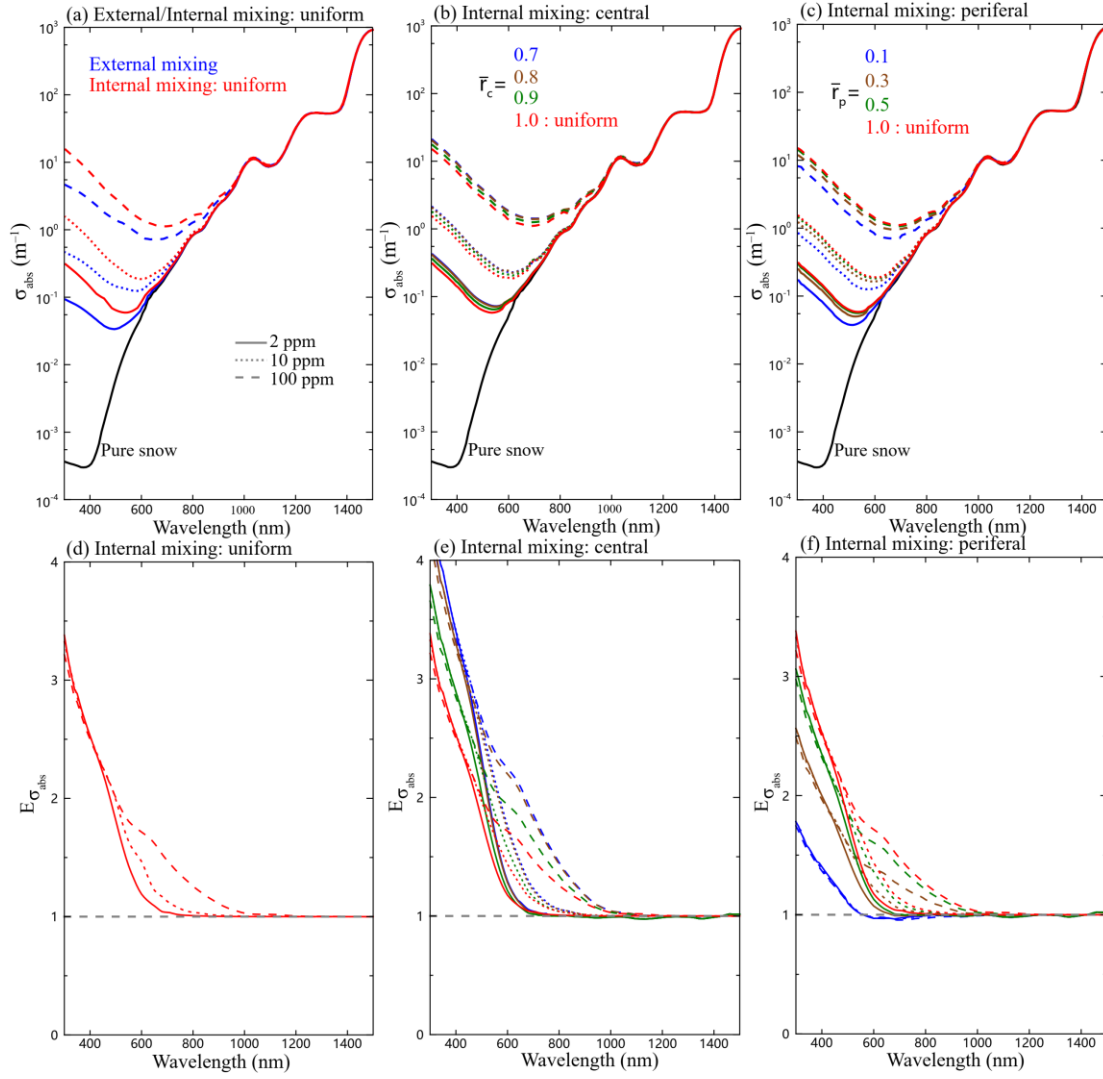
Figure 4. Snow absorption coefficients (σ_{abs}) for dust–snow (a) external and internal mixing (uniform), (b) internal mixing (central), and (c) internal mixing (peripheral), as a function of wavelength with different dust concentrations and $\overline{r_c}$ and $\overline{r_p}$. The corresponding enhancement ($E_{\sigma_{abs}}$) caused by (d) internal mixing (uniform), (e) internal mixing (central), and (f) internal mixing (peripheral) relative to external mixing, is shown as a function of wavelength. The snow grain radius was assumed to be 200 µm.
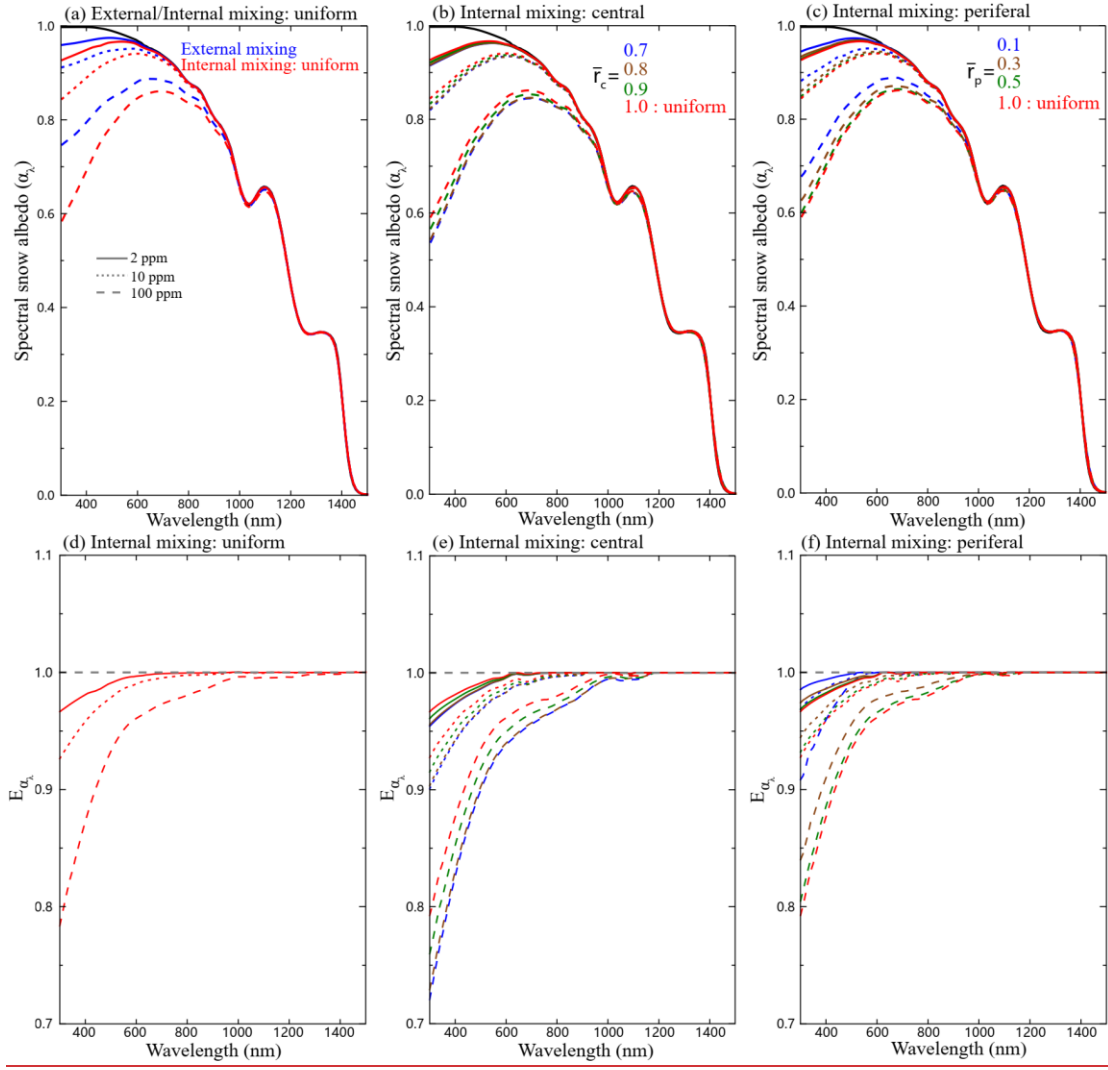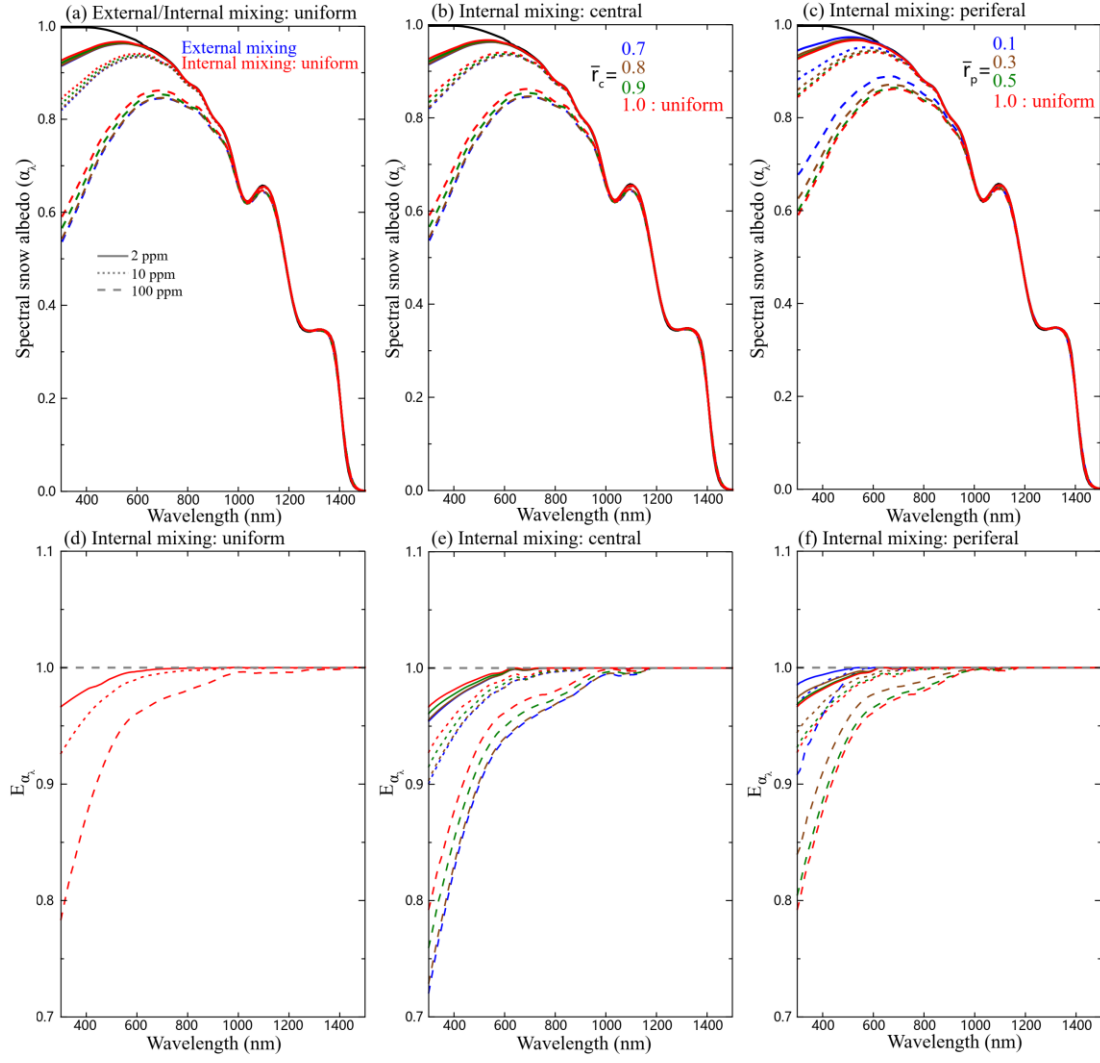
Figure 5. Same as Figure 4, but for spectral snow albedo (α_λ).
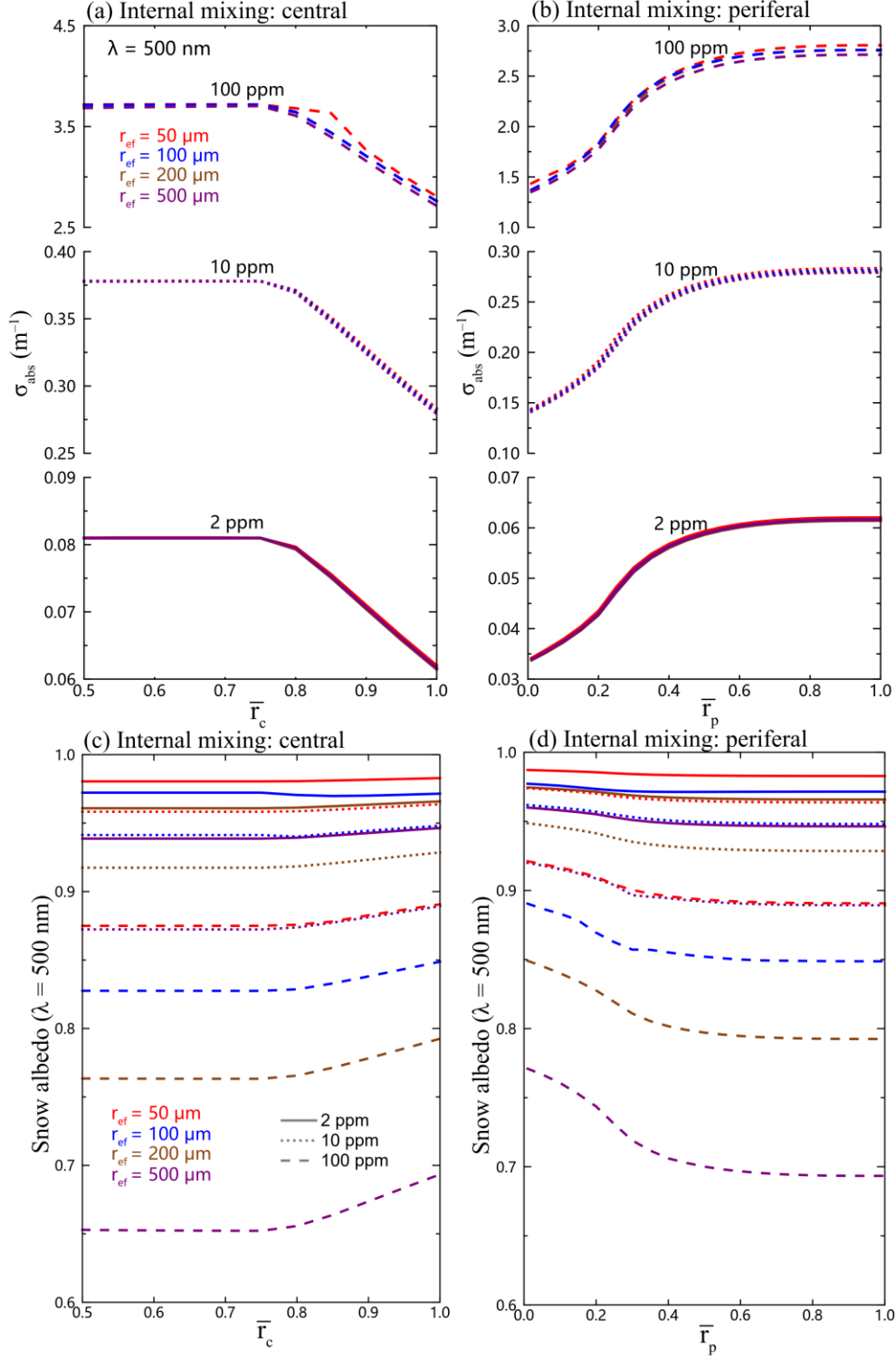
Figure 6. The snow absorption coefficient (σ_{abs}) at 500 nm wavelength as a function of $\overline{r_c}$ and $\overline{r_p}$ for (a) internal mixing (central) and (b) internal mixing (peripheral) with different snow grain radii and dust mass concentrations. (d) and (e) are the same as (a) and (b), but for snow albedo at 500 nm wavelength.
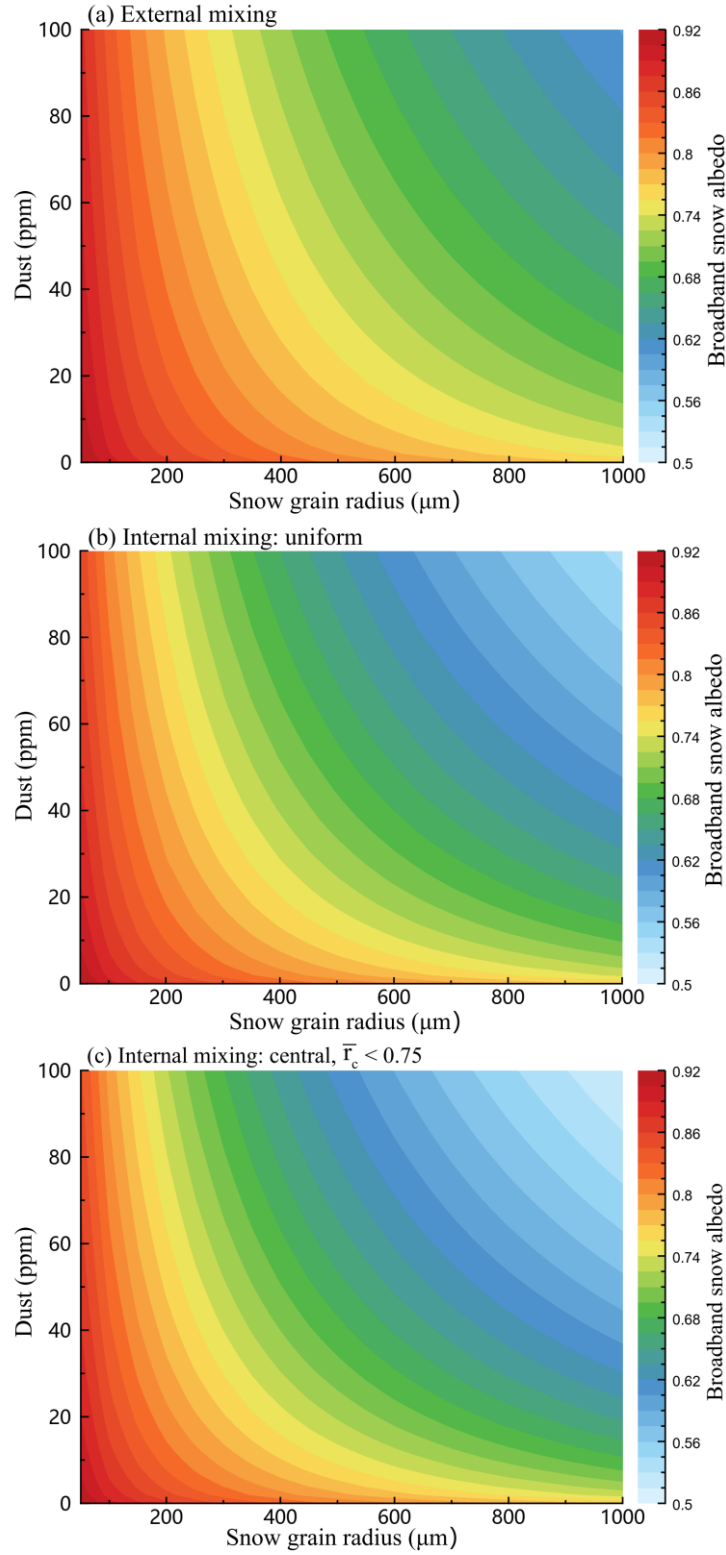
2 **Figure 7.** Broadband snow albedo ($\alpha_{integrated}$) variations affected by different dust
3 mass concentrations and snow grain radii for (a) external mixing, (b) internal mixing
4 (uniform), and (c) internal mixing (central, $\overline{r}_c$ <0.75).
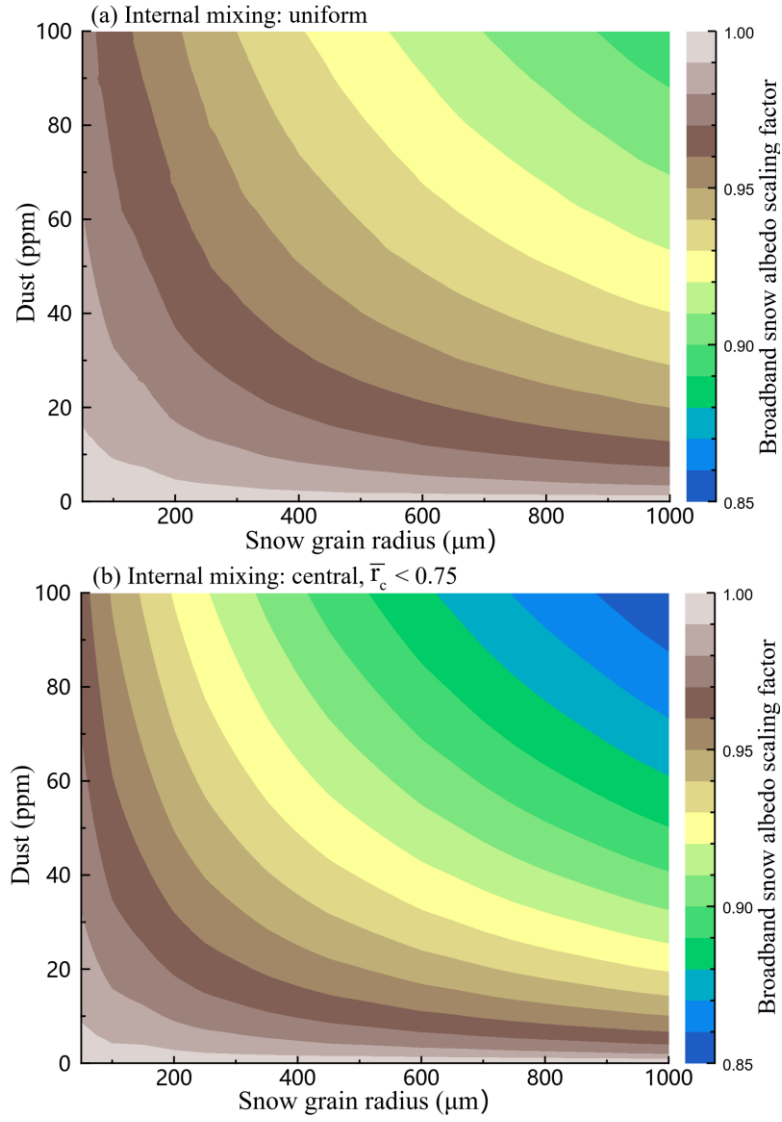
Figure 8. Variations in the broadband snow albedo scaling factor ($E_{\alpha,\ integrated}$, ratio of

$\alpha_{integrated}$ for IDM to EDM) due to different dust mass concentrations and snow grain

radii for (a) internal mixing (uniform) and (b) internal mixing (central, $\overline{r}_c$ <0.75).
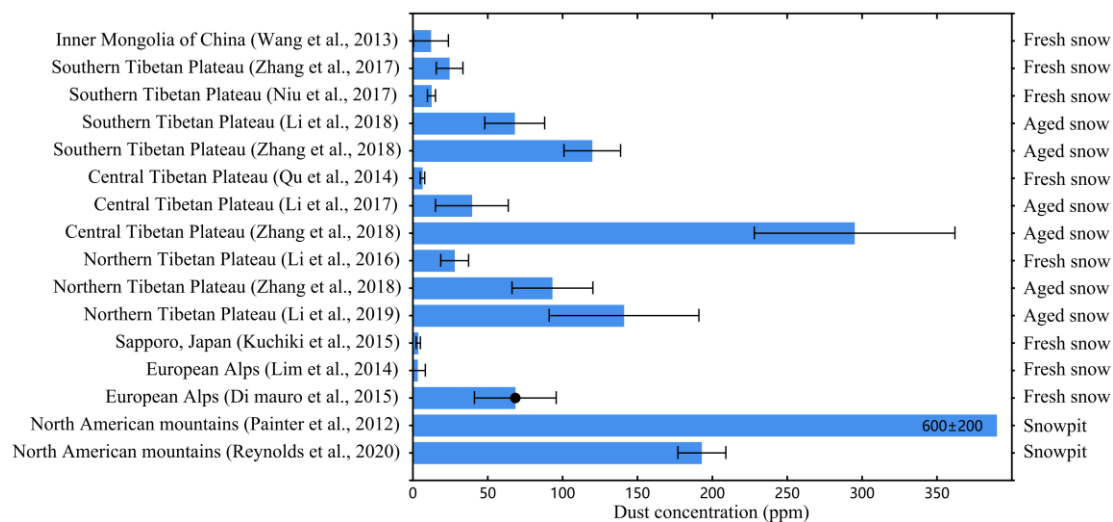
2 **Figure 9.** In situ measurements of dust concentrations in snow (fresh snow, aged snow,
3 and snowpit from field sampling in different regions of the Northern Hemisphere. The
4 solid black circle represents snow samples that were collected days after a significant
5 dust transport event.
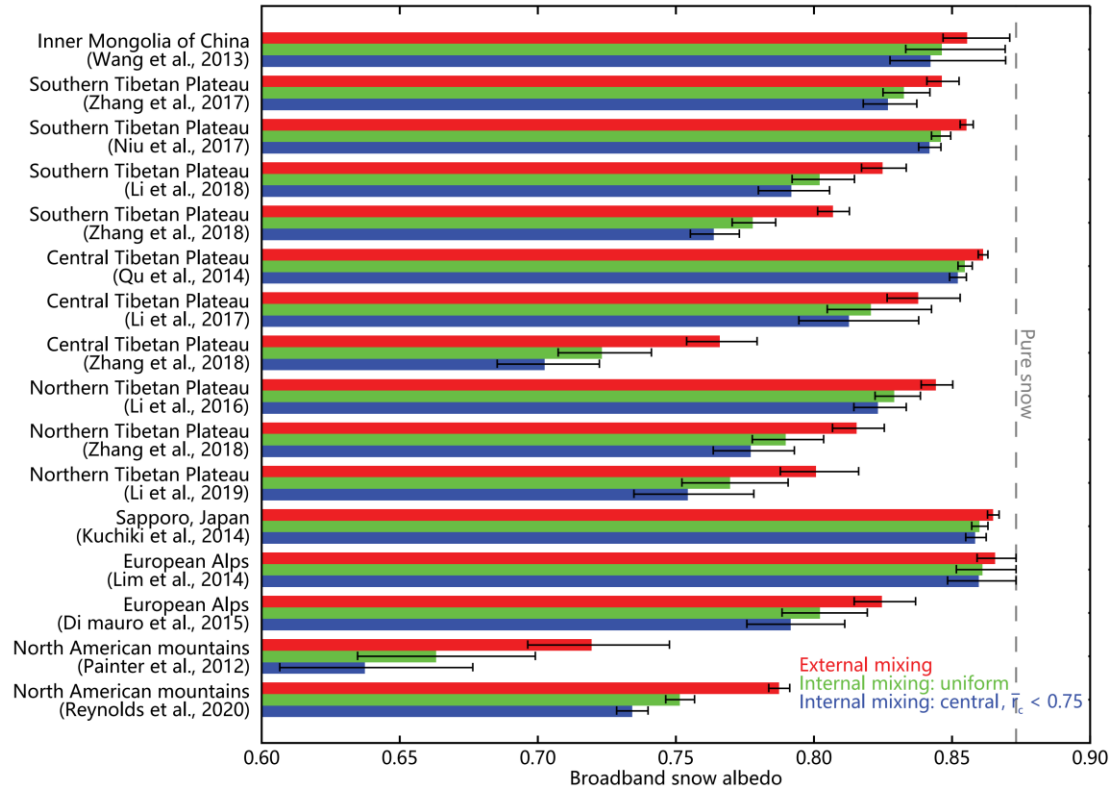
2 **Figure 10.** Calculated broadband snow albedo based on dust concentration

3 measurements in different areas for dust–snow external mixing, internal mixing

4 (uniform), and internal mixing (central, $\bar{r}_c$ <0.75). The dashed line represents

5 broadband albedo of pure snow, and the snow grain radius was assumed to be 200 µm.
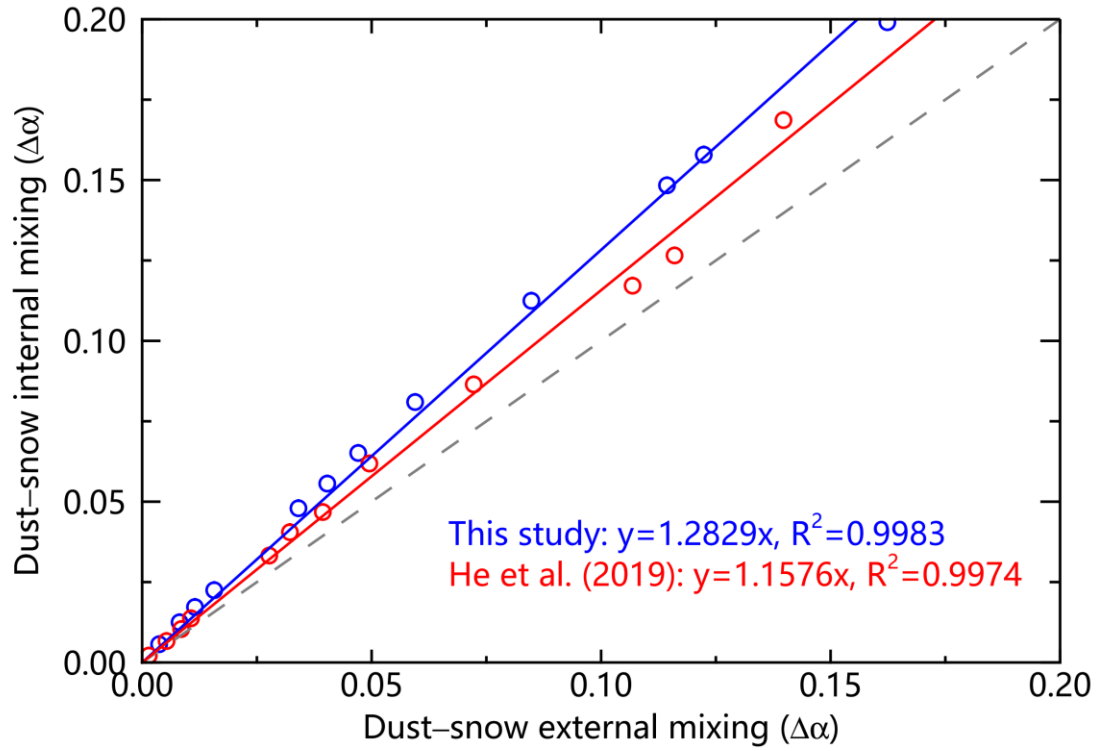
2 **Figure 11.** Comparisons of snow albedo reduction ($\Delta\alpha$) under the cloudy sky caused

3 by dust-snow uniform internal mixing (y-axis) and external mixing (x-axis) for this

4 study (blue) and He et al. (2019) (red).